TFRSAC #31

Status Update: Operational GOES-R Fire Product

Chris Schmidt

Researcher, CIMSS/SSEC/UW-Madison

29 May 2019

With Invaluable help from:
Ivan Csiszar (NOAA), Wilfrid Schroeder (NOAA), Joanne Hall (UMD), Shobha Kondragunta (NOAA), Fangjun Li (GSCE), and Xiaoyang Zhang (GSCE)

ABI Fire Detection Current Status

The Fire Detection and Characterization Algorithm (FDCA) is NOAA's baseline GOES-R fire detection algorithm

Product resolution is 2 km and provides fire detections, fire radiative power (FRP), fire size, and fire temperature

FRP is now provided for all detected fire classes; size and temperature only provided for highest confidence fires

NOAA runs the FDCA on the 5 minute CONUS and 10 minute Full Disk sectors only

As of 29 May 2019 it is Provisional for GOES-16 (available through AWIPS, PDA, and on CLASS) and Beta for GOES-17 (not publicly available, Provisional status expected in early July 2019)

The GOES-17 "Loop heat pipe anomaly" reduces FDCA performance by making fires harder to find, but generally does not create false alarms (but it can)

GOES-17 mitigation measures are being developed and expected to be deployed in late 2019

Product quality assessments/validation is under way

ABI Fire Detection

Context of algorithm development: Fire detection has a very wide range of users, from aerosol modelers with a high tolerance for false alarms to the emergency managers responsible for deploying personnel who have a low tolerance for false alarms to public and private users who seek the fastest detections possible with varying requirements for accuracy to broadcast media to NWS forecasters and more. The ABI Fire Detection and Characterization Algorithm (FDCA, aka Fire Hot-Spot [FHS]) seeks to serve the needs of as many these users as possible. It was built from the Wildfire Automated Biomass Burning Algorithm (WFABBA) used with the old GOES satellites.

The ABI FDCA provides 2 km fire detection and characterization data for the five minute CONUS and ten minute Full Disk scans. The one minute mesoscale sectors are not produced operationally at this time, but that could change if sufficient demand arises. (If you want it, ask for it)

The algorithm is contextual, it considers a candidate fire pixel in comparison to its neighbors, but there are some fixed thresholds involved. FDCA performs its own opaque cloud screening: fires will shine through optically thin clouds and speed is of the essence, so sources of latency and product pre-requisites were reduced or eliminated if possible. It also accounts for surface emissivity and atmospheric attenuation of the fire signal by water vapor in the atmosphere.

ABI Fire Characterization

While fire detection is important, quantitative applications such as smoke modeling need to know how energetic the fire is. The original ABBA was designed to provide fire size and fire temperature using a relationship described by Matson and Dozier that correlated the fire temperature and pixel fraction with the observed radiances in the ~4 μm and ~11 μm bands. Later on, fire radiative power (FRP) caught on as a simplified way to assess a fire's character.

Due to the subpixel nature of fires:

- The Dozier Method and FRP are describing a hypothetical, uniform fire with those properties that produces the same radiance signature
- *The size should not be taken literally*
- FRP is the best proxy for intensity

Fire in the ABI Bands

Camp Fire
8 Nov 2018
8:02 AM PST – 5:57 PM PST

All 16 bands, dynamically scaled so there is some flickering and noise is amplified at times.

Fire signal in many, but not all bands (and not visible in bands 1-4, though fires can appear in bands 3 and 4 at night)

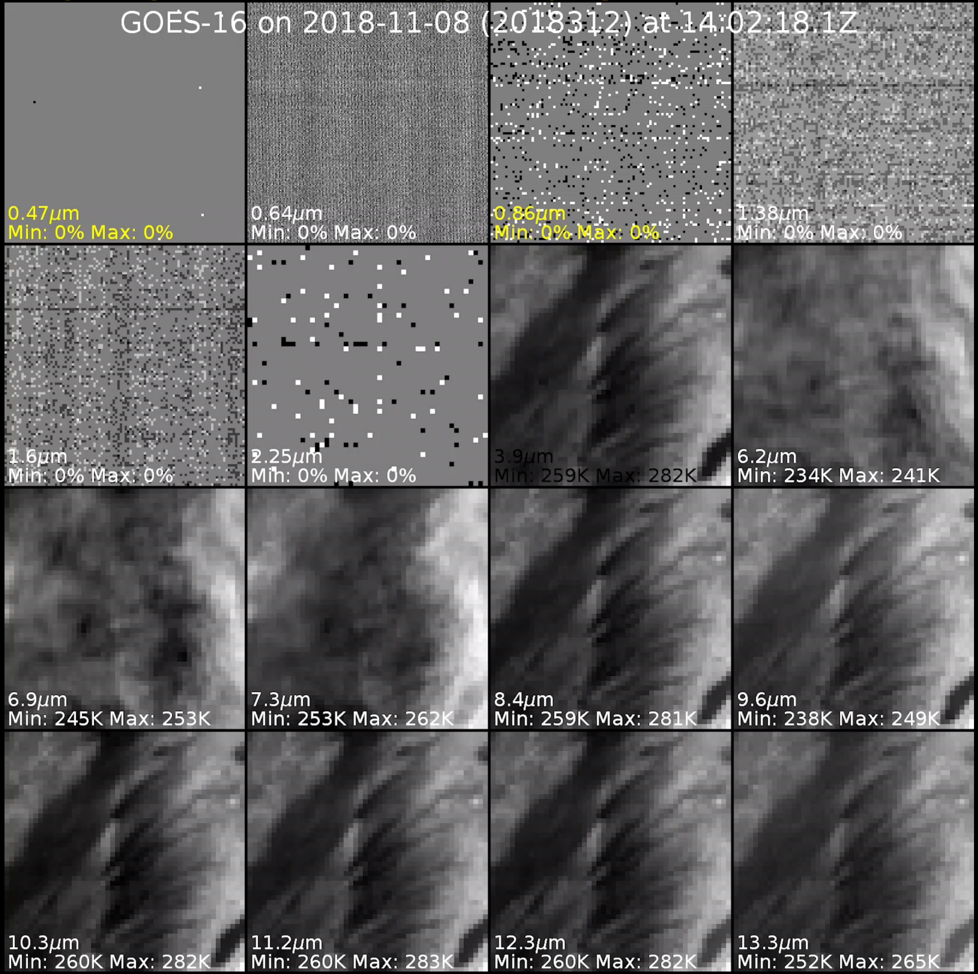

Sensitivity and Detection: The Camp Fire

On 8 November 2018, at about 6:30 AM PST, the fire that would shortly destroy Paradise, CA and overtake the Tubbs Fire as California's worst, began. GOES-17 data was unavailable as the satellite was drifting to its station at 135.2°W, but GOES-16 could see the area, albeit at an angle into a relatively hilly region.

Despite the less than ideal view angle and relative position, GOES-16 first noted a heat signature at 6:22 AM PST (14:22 UTC), though the algorithm did not identify it as a fire until later. GOES-16 ABI only provided five minute imagery, however. Under normal circumstances GOES-17 would provide one minute imagery over that region by default.

The Camp Fire

GOES-16
2018-11-08 (2018312)
14:02:18.1Z

Early hours of the Camp Fire on 8 November 2018.

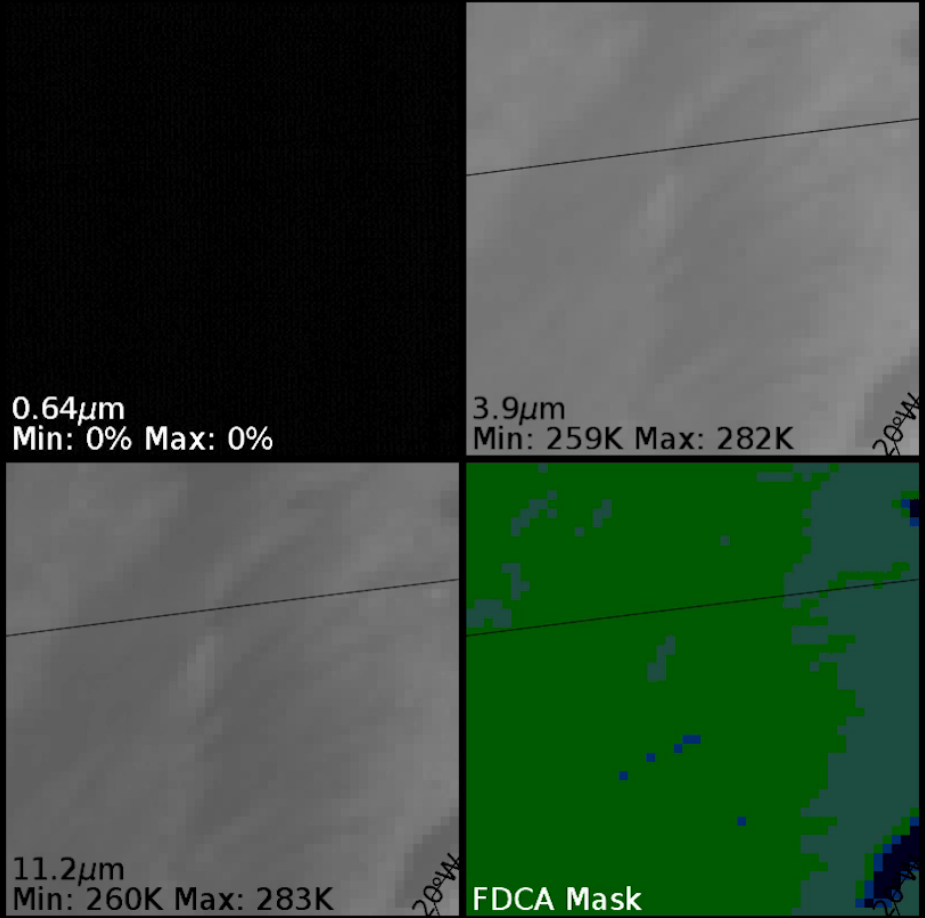

Fire Temperature RGB

Fire Legend

- Processed Fire
- High Possibility Fire
- Saturated Fire
- Medium Possibility Fire
- Cloudy Fire
- Low Possibility Fire
- Fire-free ground
- Cloudy (BT based)
- Cloudy (Rad Diff, night)
- Cloudy (Rad Diff, day)
- Background Calc Failed
- Water

The Camp Fire

GOES-16
2018-11-08 (2018312)
14:32:18.1Z

Early hours of the Camp Fire on 8 November 2018.

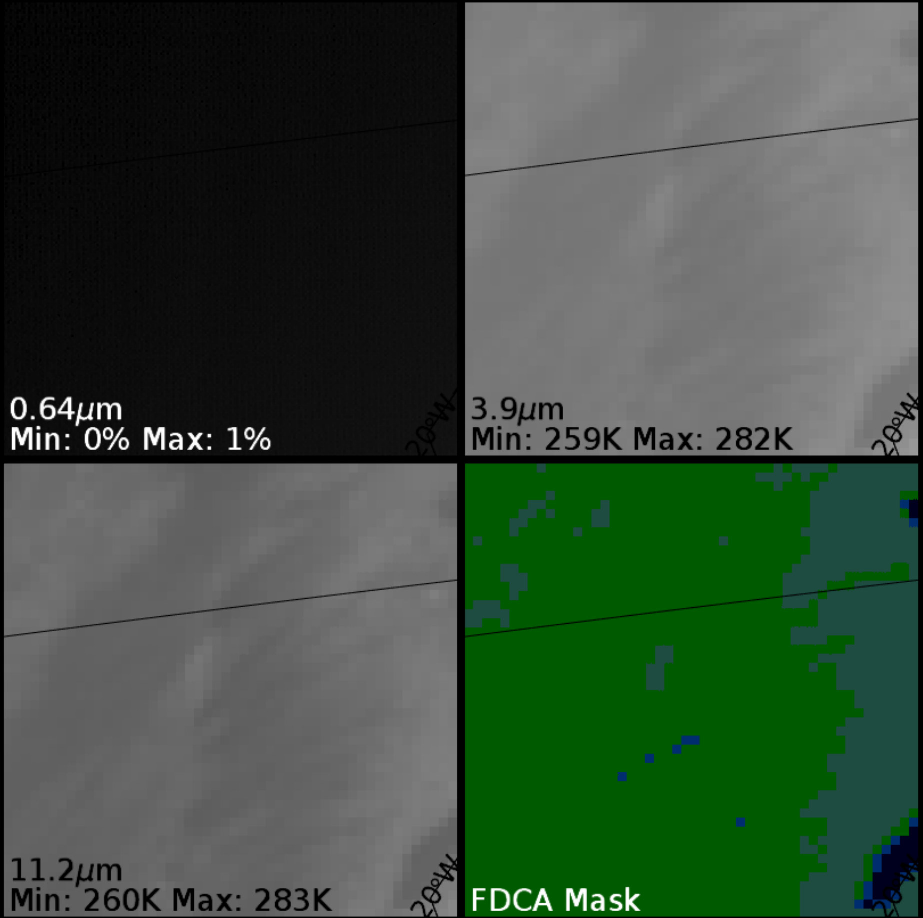

Fire Temperature RGB

Fire Legend
- Processed Fire
- High Possibility Fire
- Saturated Fire
- Medium Possibility Fire
- Cloudy Fire
- Low Possibility Fire
- Fire-free ground
- Cloudy (BT based)
- Cloudy (Rad Diff, night)
- Cloudy (Rad Diff, day)
- Background Calc Failed
- Water

The Camp Fire

GOES-16
2018-11-08 (2018312)
14:37:18.1Z

Early hours of the Camp Fire on 8 November 2018.

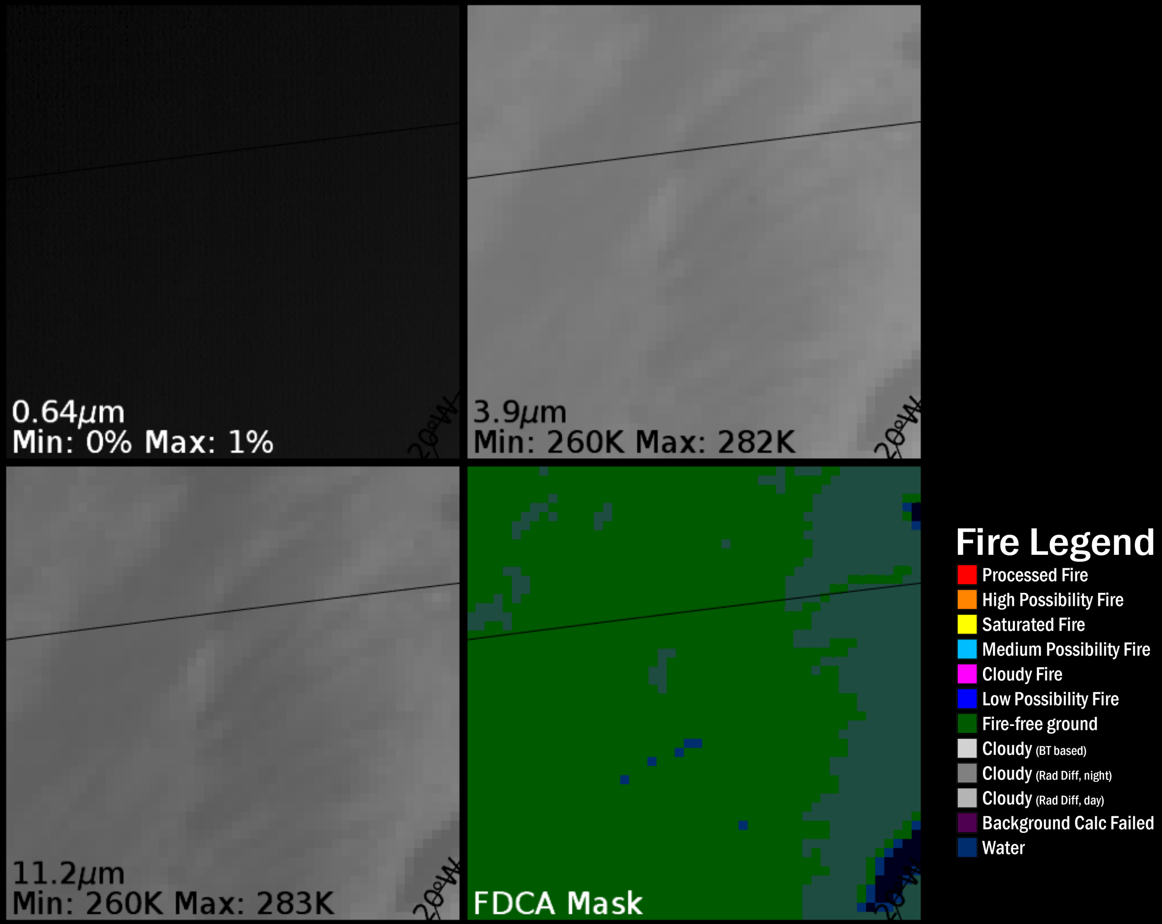

Fire Temperature RGB

The Camp Fire

Early hours of the Camp Fire on 8 November 2018.

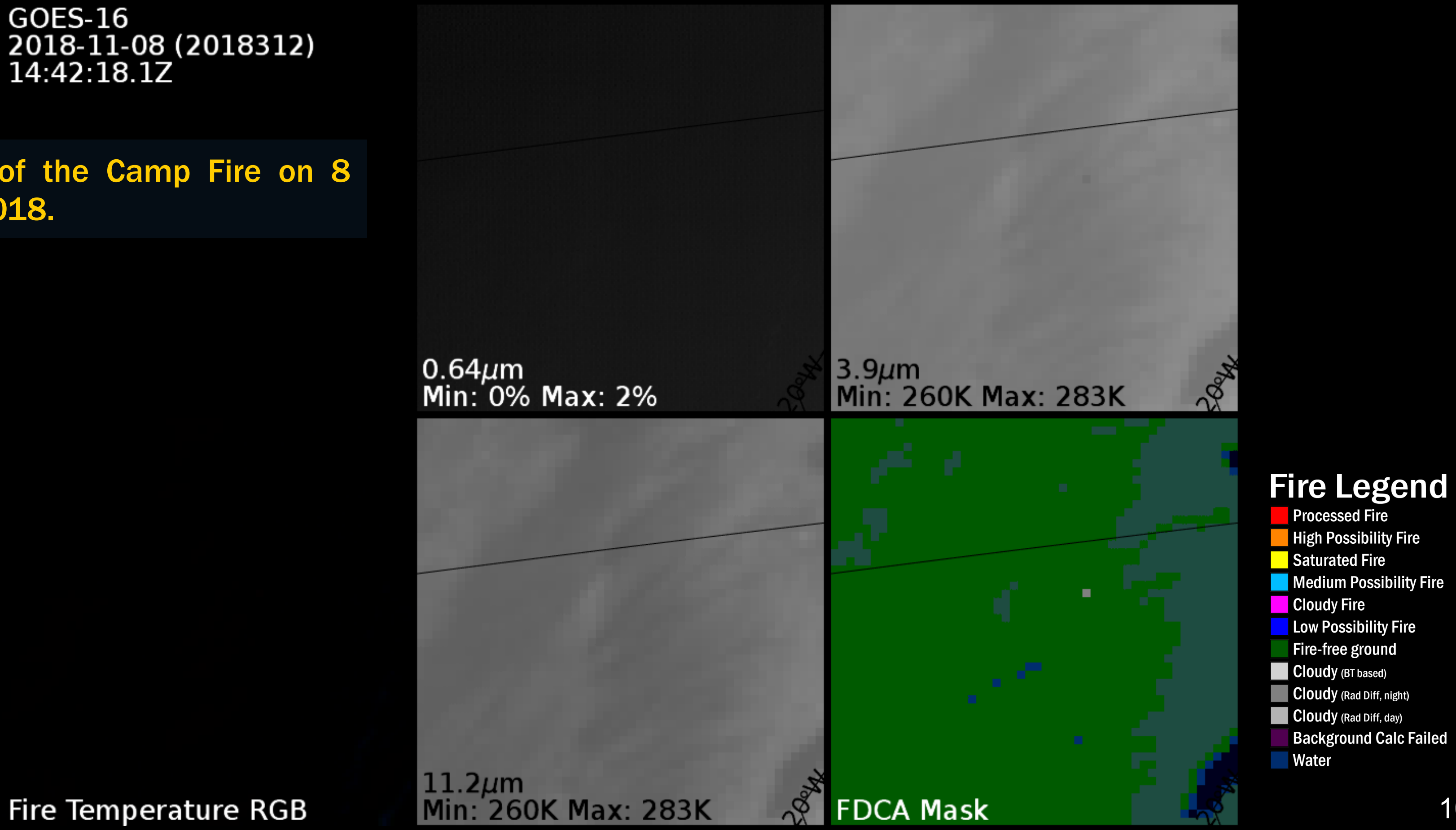

The Camp Fire

GOES-16
2018-11-08 (2018312)
14:47:18.1Z

Early hours of the Camp Fire on 8 November 2018.

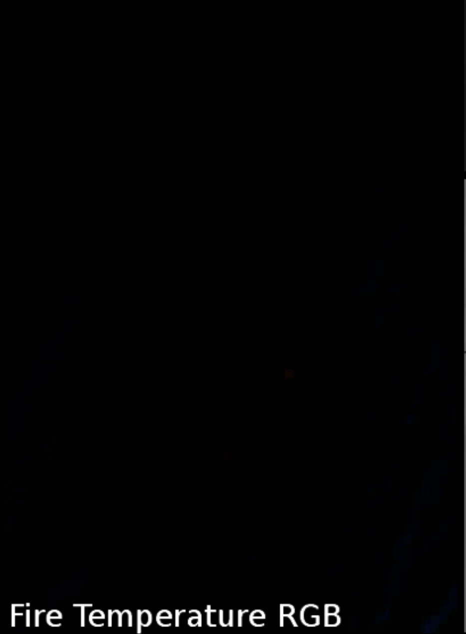

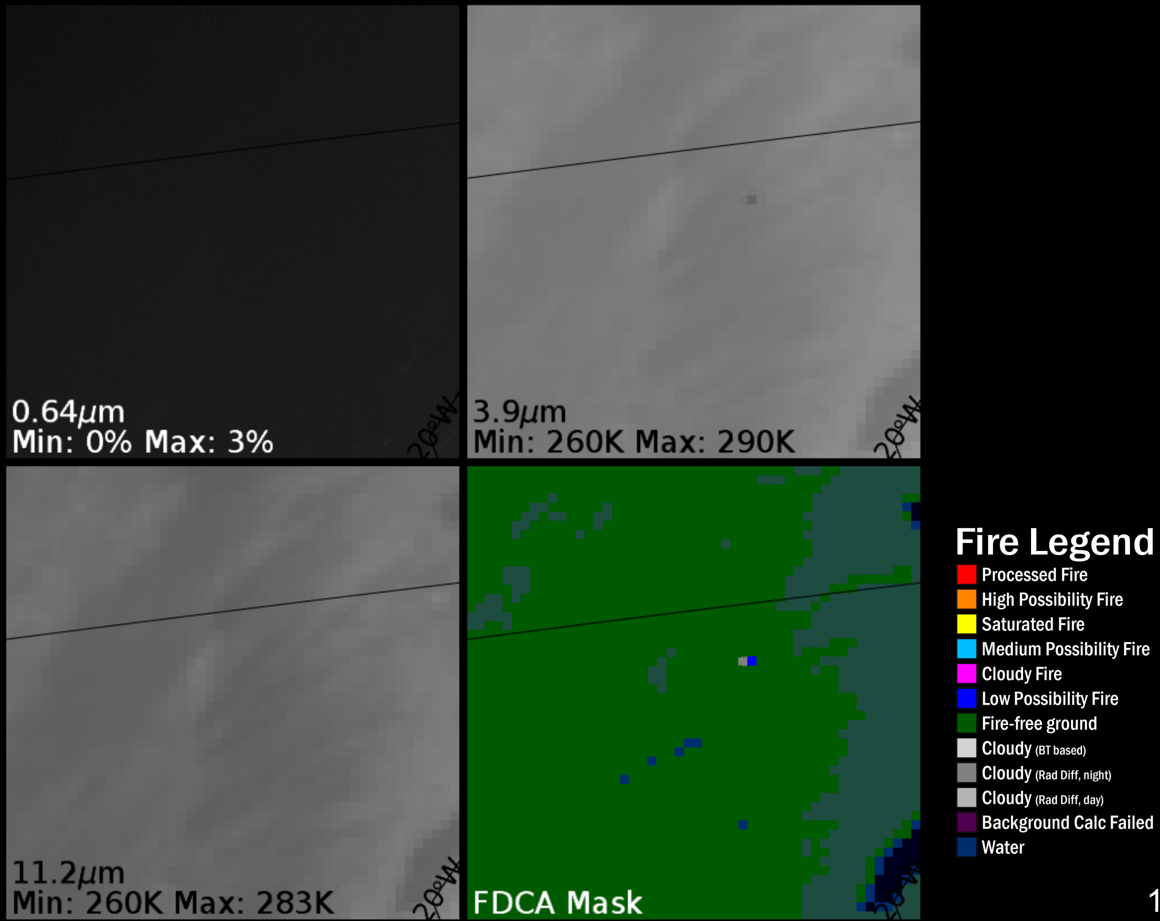

The Camp Fire

GOES-16
2018-11-08 (2018312)
14:52:18.1Z

Early hours of the Camp Fire on 8 November 2018.

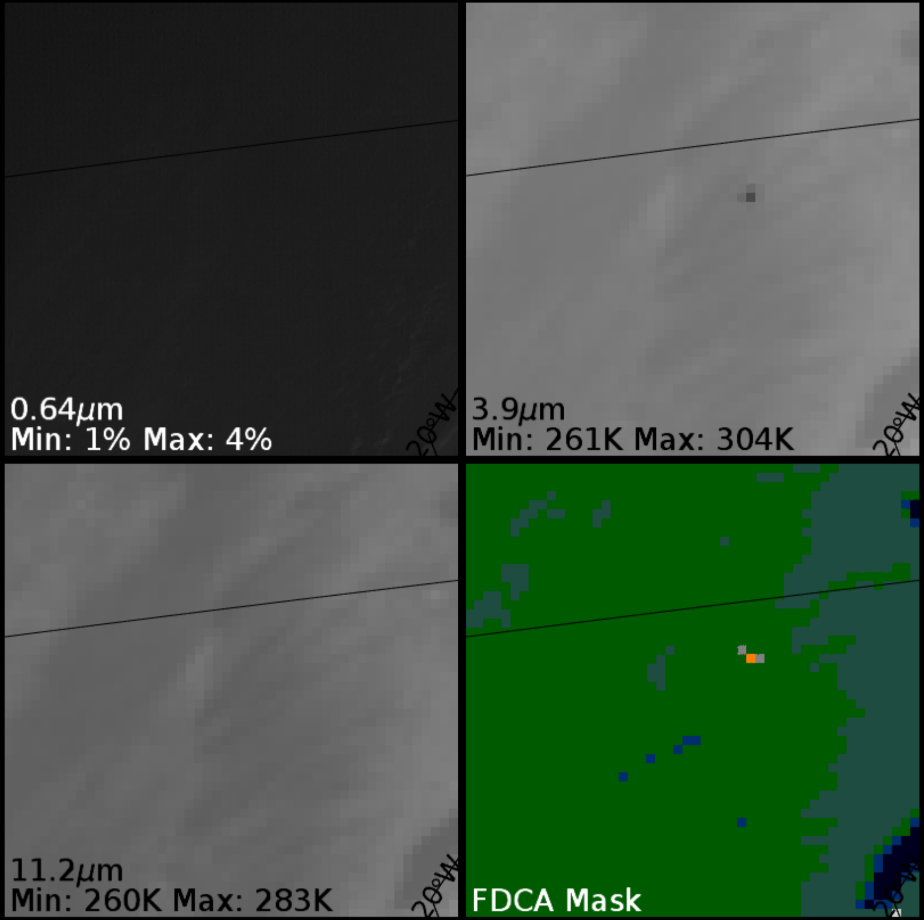

Fire Legend

- Processed Fire
- High Possibility Fire
- Saturated Fire
- Medium Possibility Fire
- Cloudy Fire
- Low Possibility Fire
- Fire-free ground
- Cloudy (BT based)
- Cloudy (Rad Diff, night)
- Cloudy (Rad Diff, day)
- Background Calc Failed
- Water

The Camp Fire

Early hours of the Camp Fire on 8 November 2018.

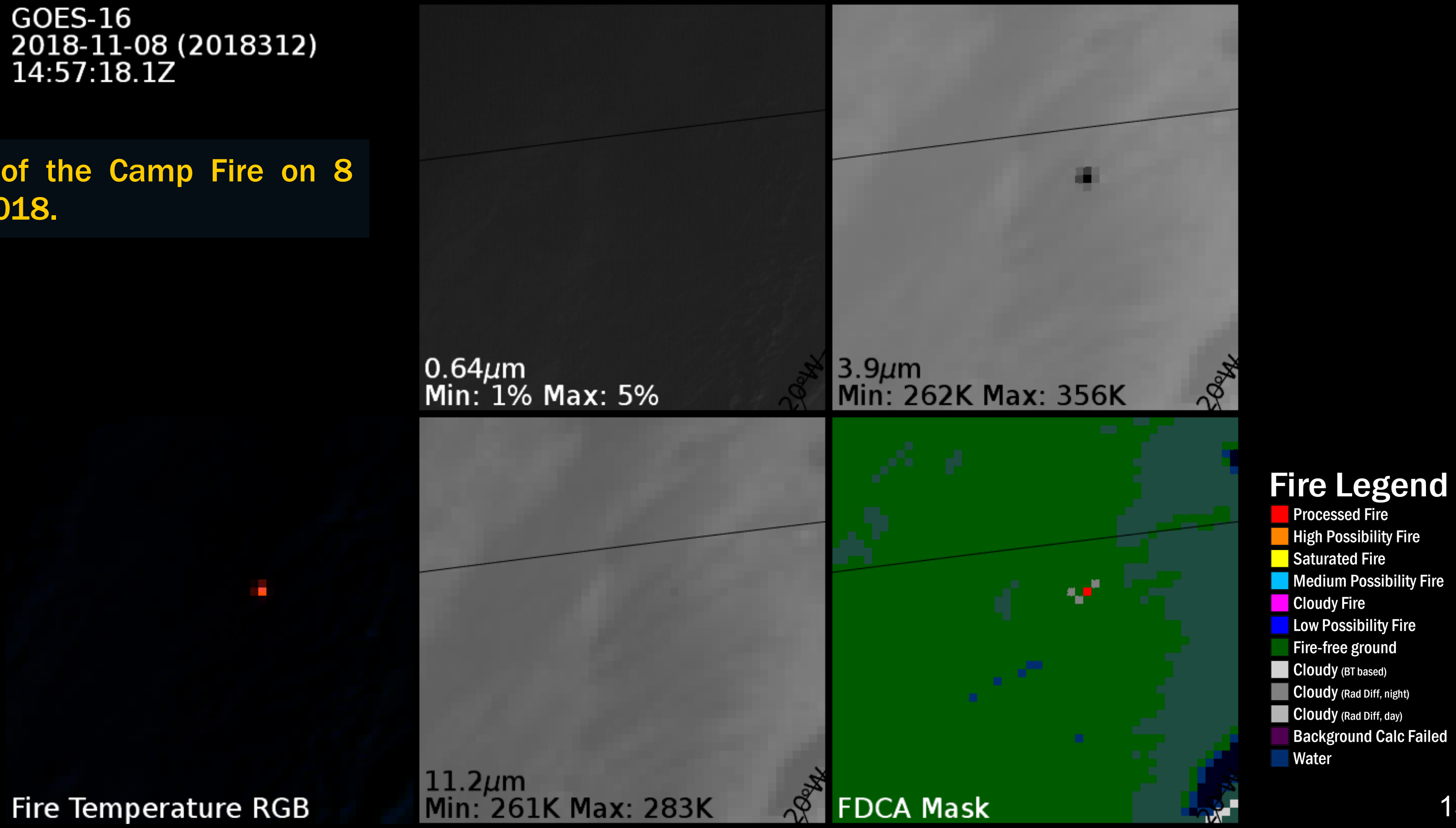

The Camp Fire

Early hours of the Camp Fire on 8 November 2018.

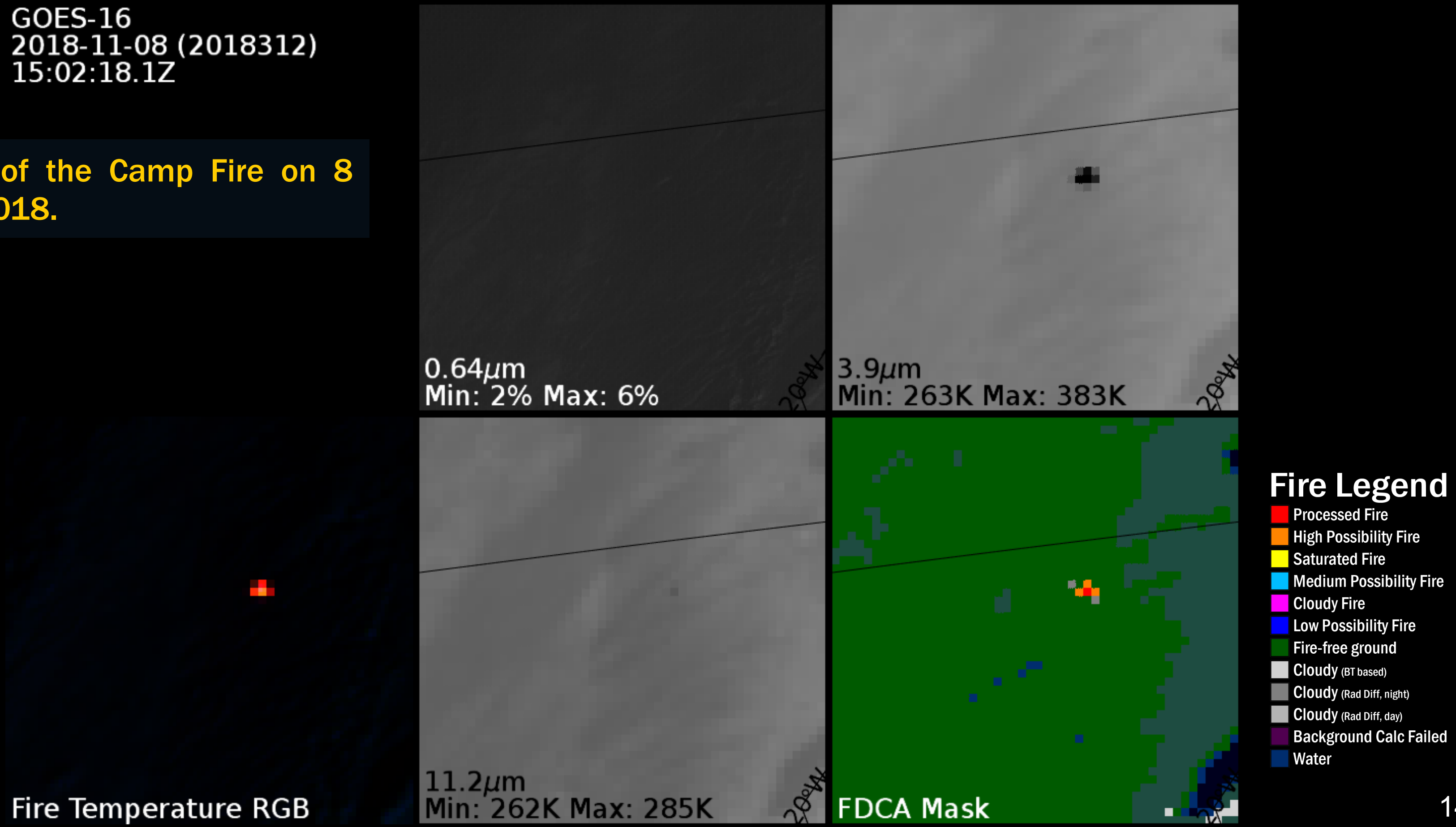

The Camp Fire

The visible, 3.9 μm, 11.2 μm, 3.9 μm minus 11.2 μm radiance difference in 3.9 μm radiance space, and FDCA fire temperature, size, and power are dynamically scaled to the minima and maxima of the data.

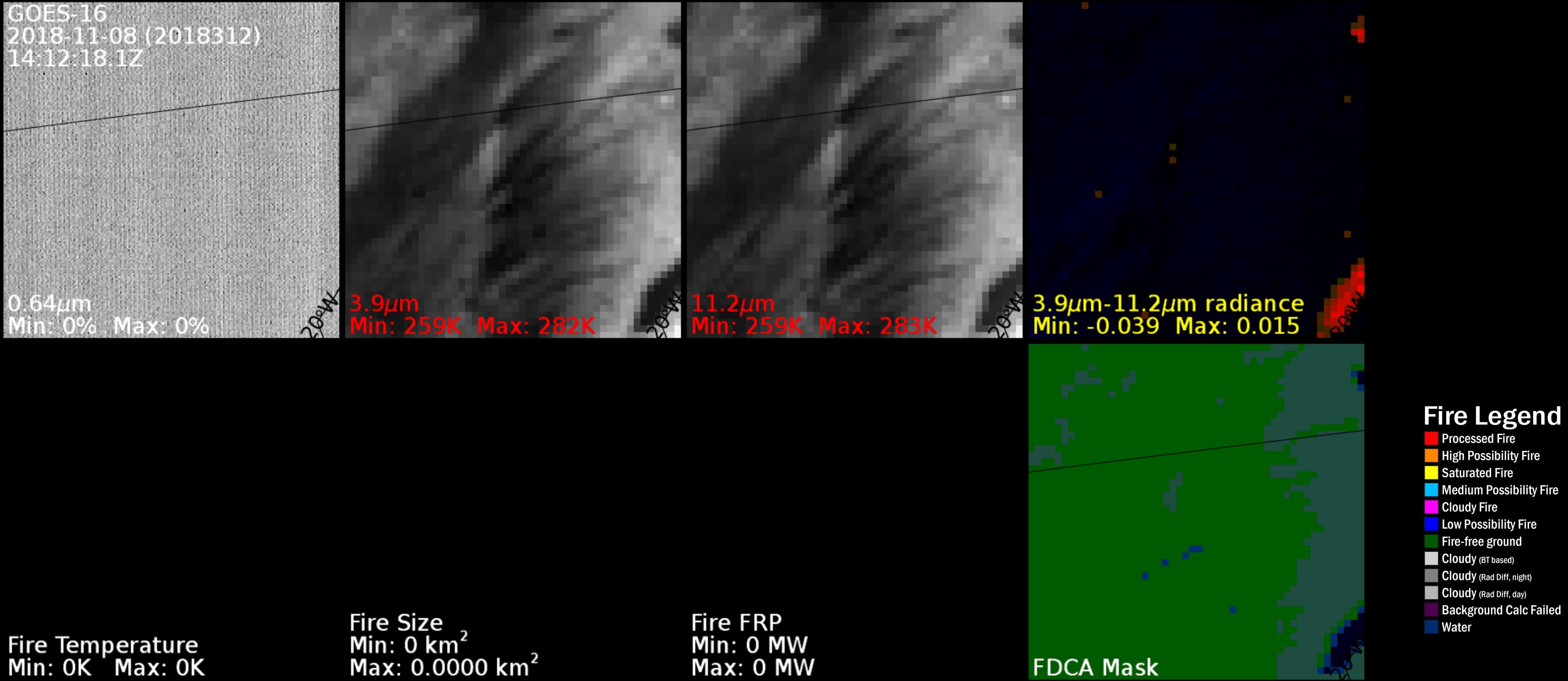

The Camp Fire

The visible, 3.9 µm, 11.2 µm, 3.9 µm minus 11.2 µm radiance difference in 3.9 µm radiance space, and FDCA fire temperature, size, and power are dynamically scaled to the minima and maxima of the data.

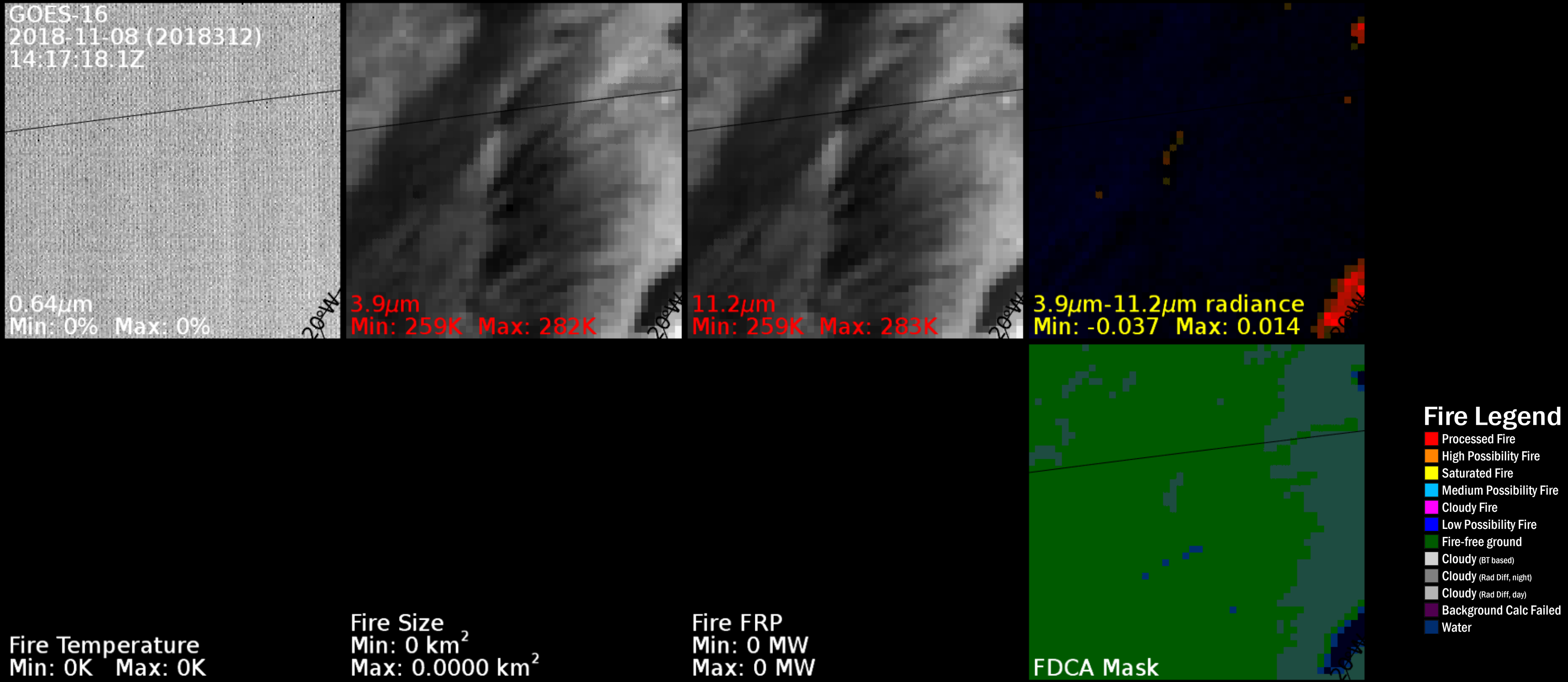

The Camp Fire

The visible, 3.9 µm, 11.2 µm, 3.9 µm minus 11.2 µm radiance difference in 3.9 µm radiance space, and FDCA fire temperature, size, and power are dynamically scaled to the minima and maxima of the data.

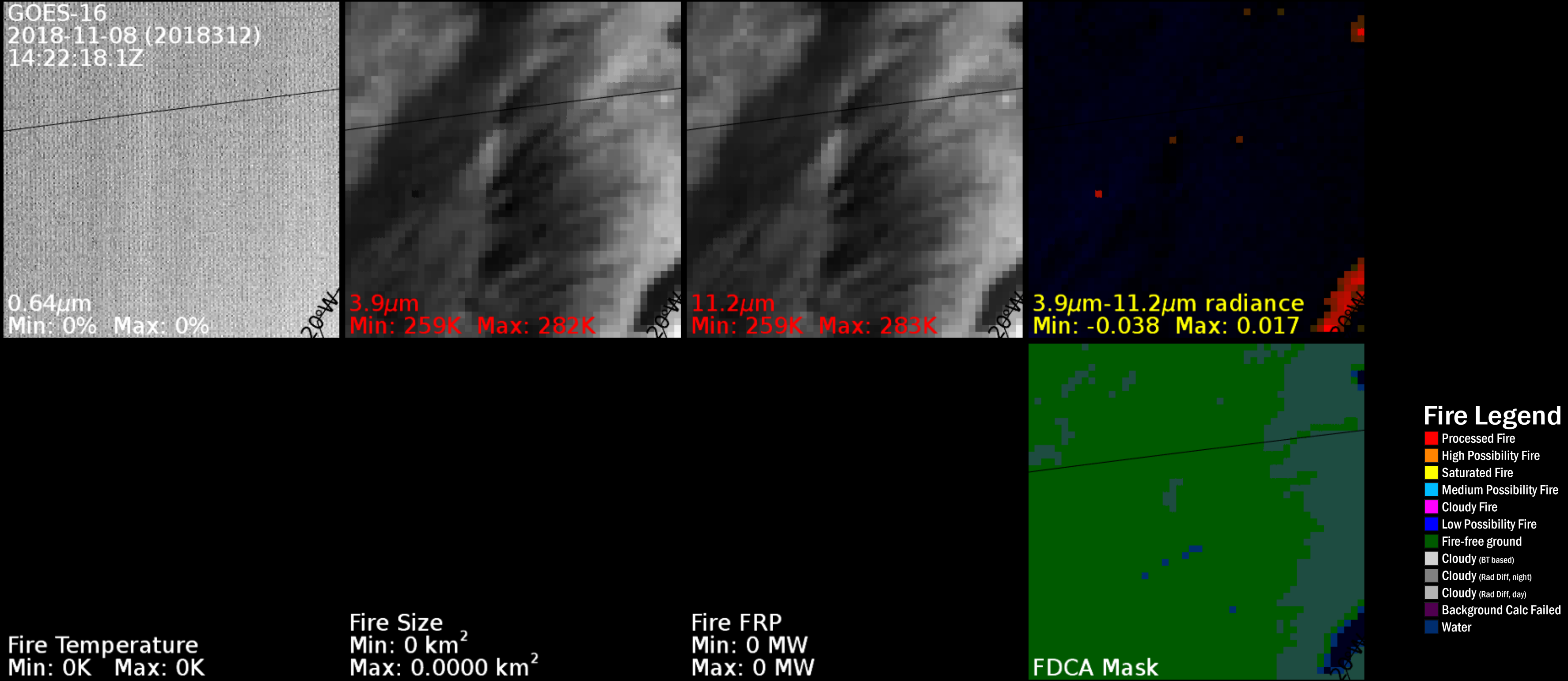

The Camp Fire

The visible, 3.9 µm, 11.2 µm, 3.9 µm minus 11.2 µm radiance difference in 3.9 µm radiance space, and FDCA fire temperature, size, and power are dynamically scaled to the minima and maxima of the data.

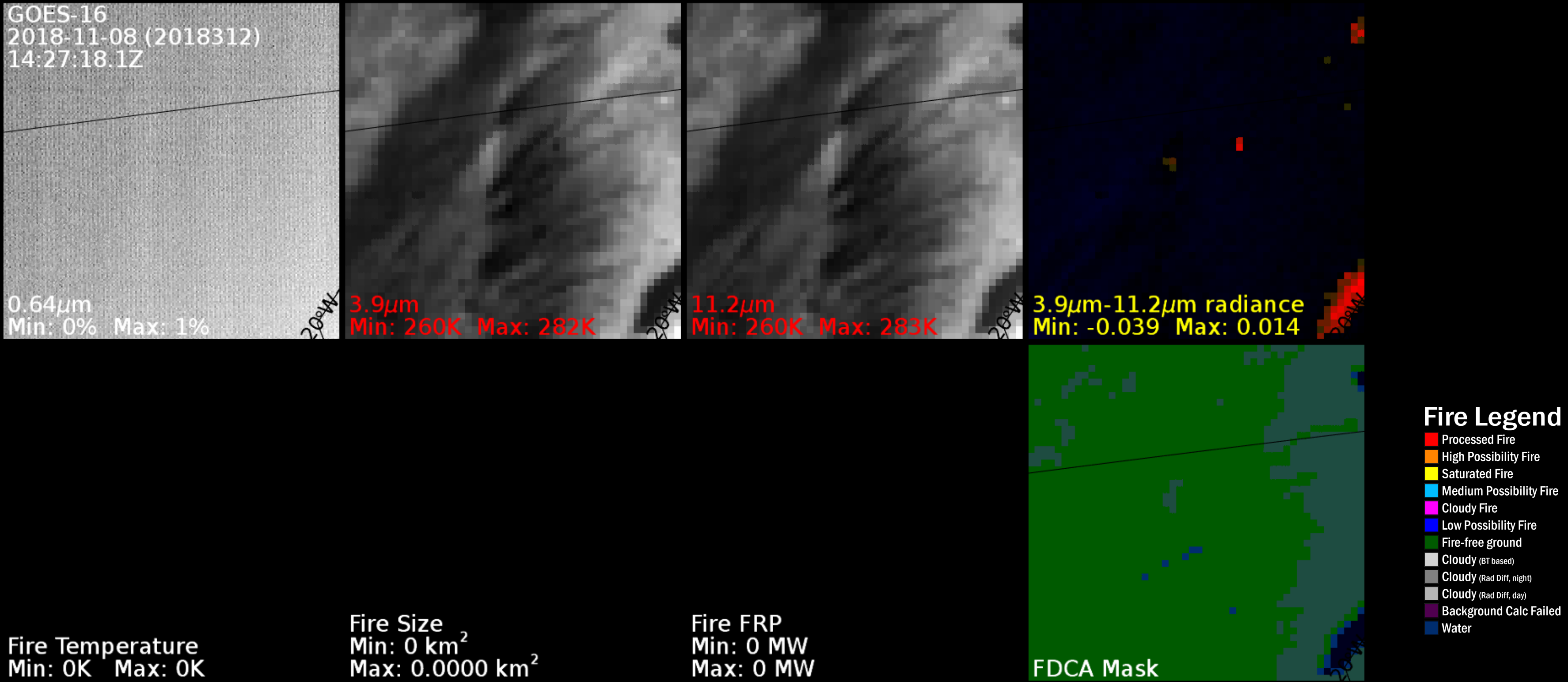

The Camp Fire

The visible, 3.9 µm, 11.2 µm, 3.9 µm minus 11.2 µm radiance difference in 3.9 µm radiance space, and FDCA fire temperature, size, and power are dynamically scaled to the minima and maxima of the data.

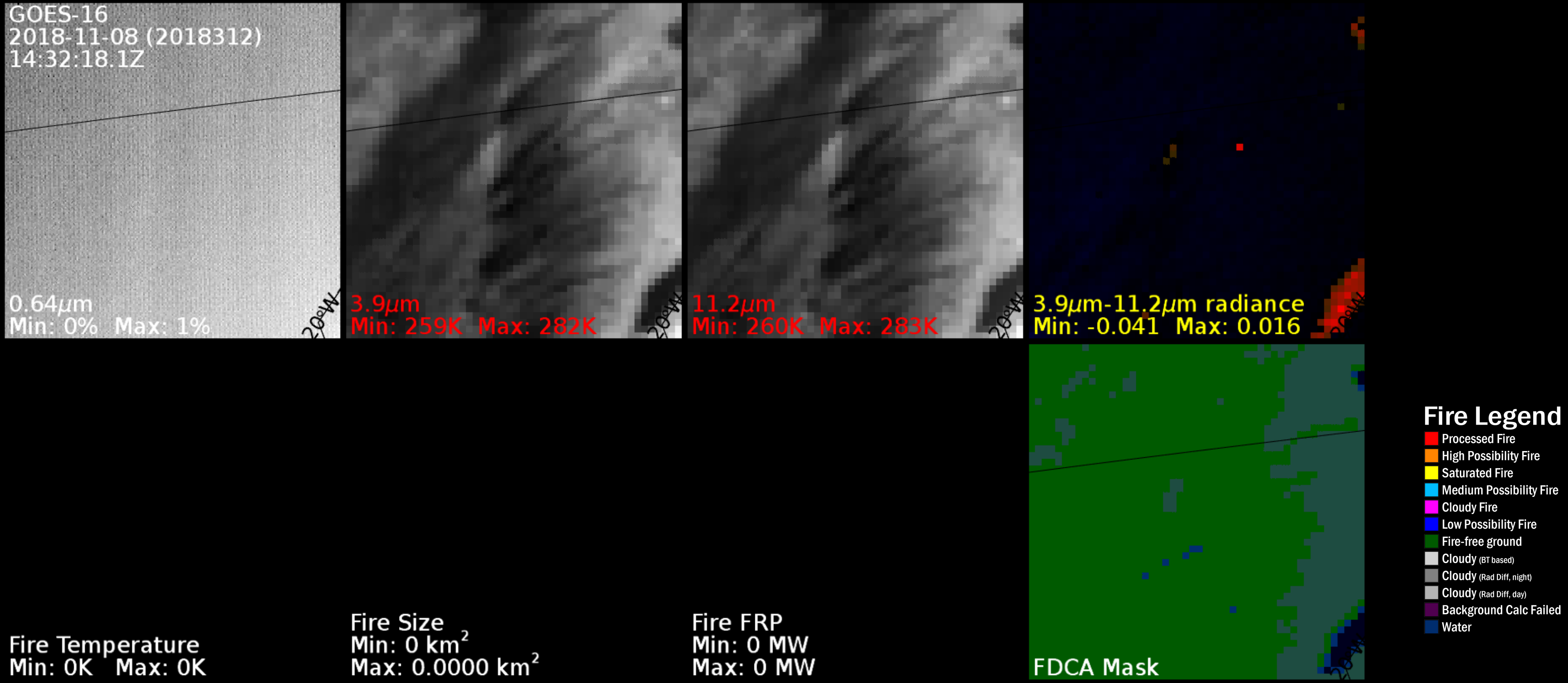

The Camp Fire

The visible, 3.9 μm, 11.2 μm, 3.9 μm minus 11.2 μm radiance difference in 3.9 μm radiance space, and FDCA fire temperature, size, and power are dynamically scaled to the minima and maxima of the data.

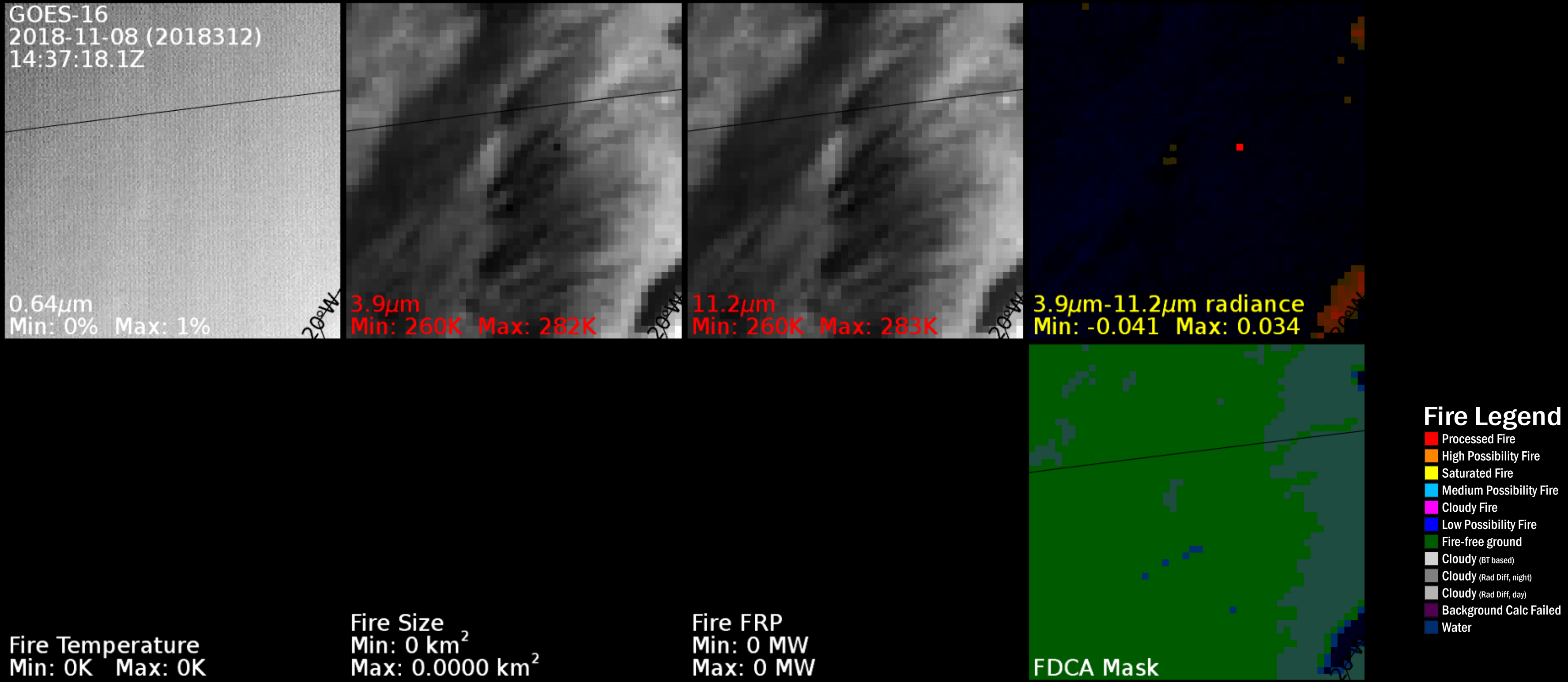

The Camp Fire

The visible, 3.9 μm, 11.2 μm, 3.9 μm minus 11.2 μm radiance difference in 3.9 μm radiance space, and FDCA fire temperature, size, and power are dynamically scaled to the minima and maxima of the data.

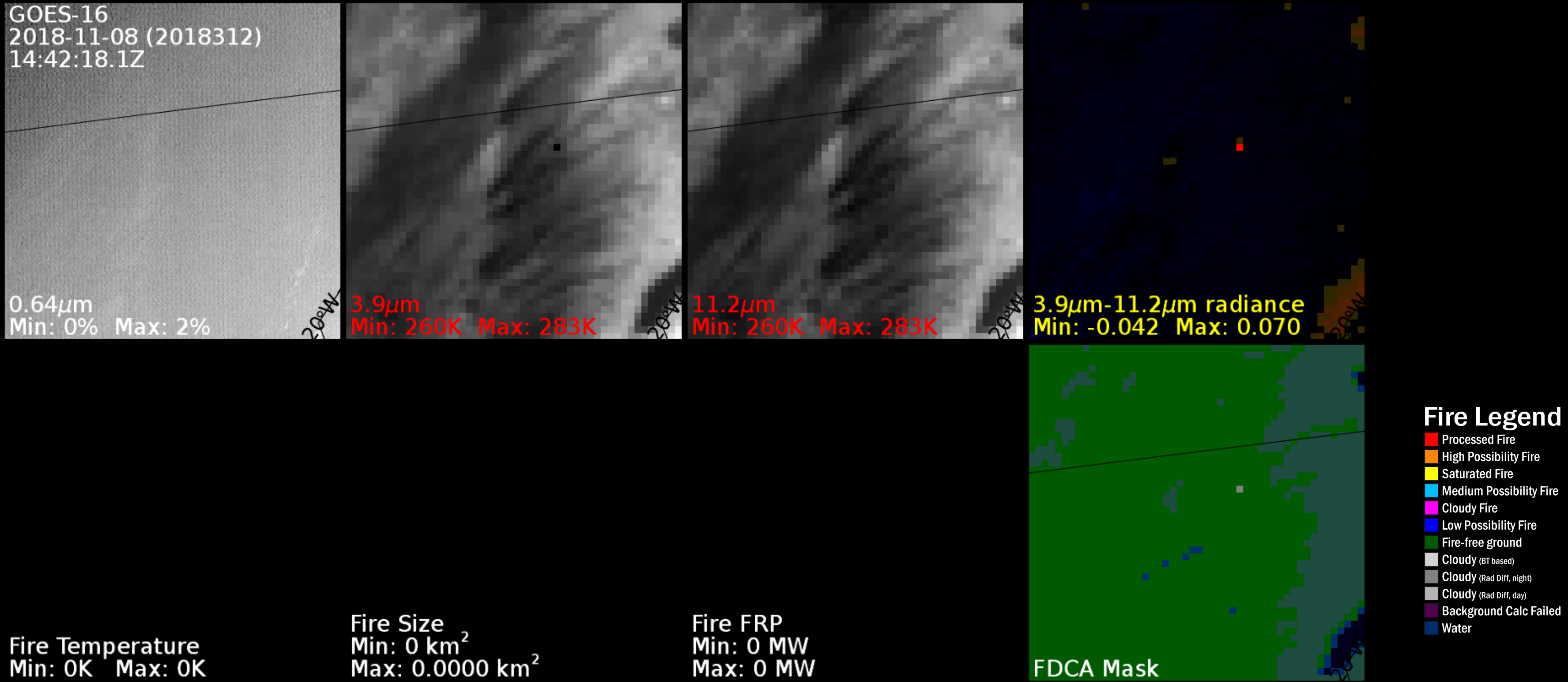

The Camp Fire

The visible, 3.9 µm, 11.2 µm, 3.9 µm minus 11.2 µm radiance difference in 3.9 µm radiance space, and FDCA fire temperature, size, and power are dynamically scaled to the minima and maxima of the data.

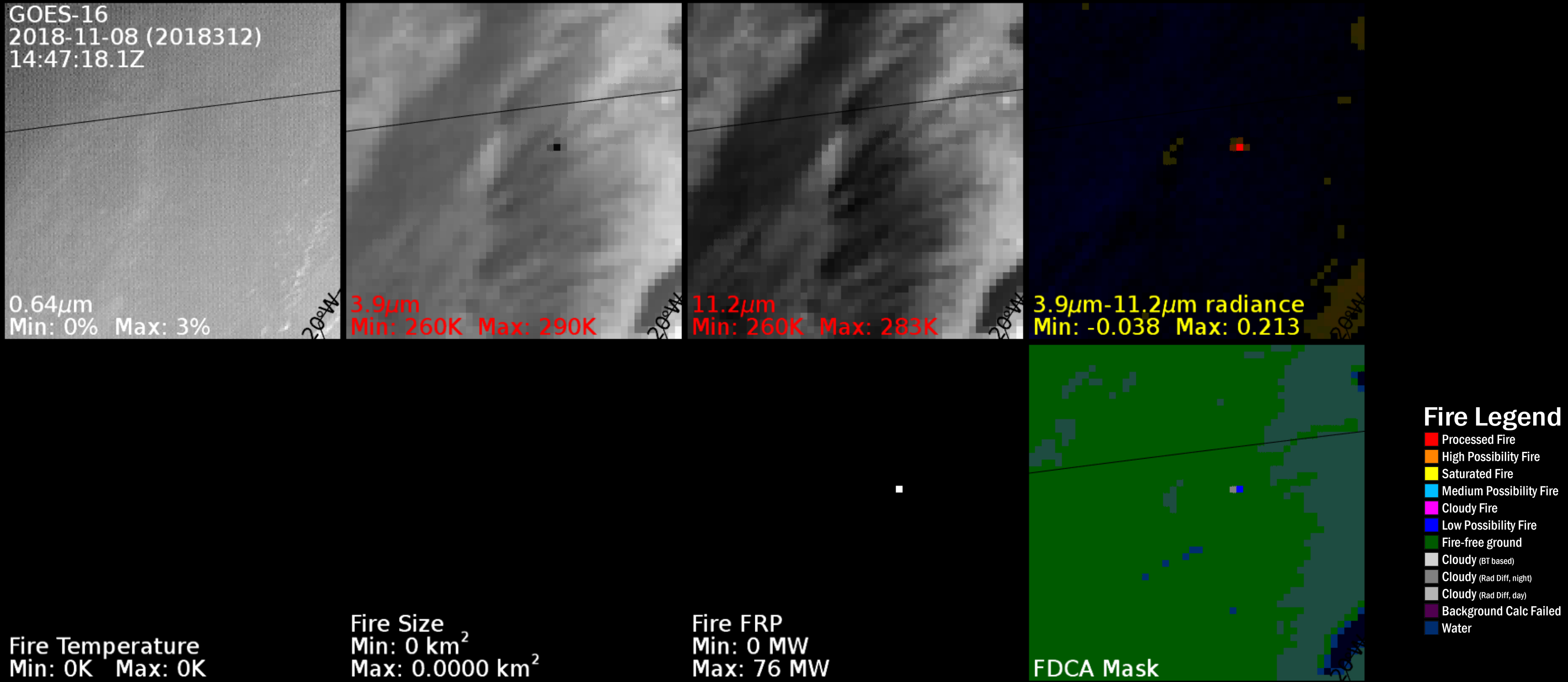

The Camp Fire

The visible, 3.9 µm, 11.2 µm, 3.9 µm minus 11.2 µm radiance difference in 3.9 µm radiance space, and FDCA fire temperature, size, and power are dynamically scaled to the minima and maxima of the data.

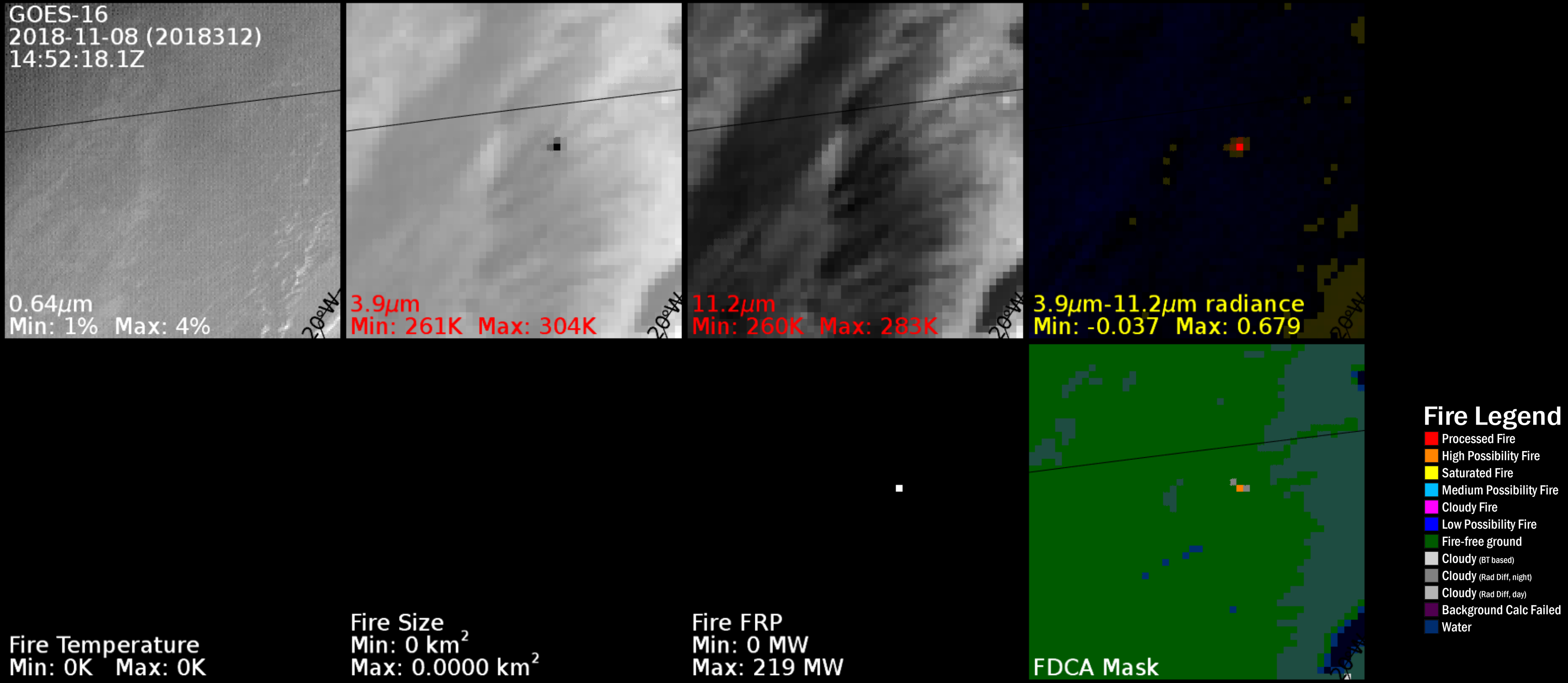

The Camp Fire

The visible, 3.9 µm, 11.2 µm, 3.9 µm minus 11.2 µm radiance difference in 3.9 µm radiance space, and FDCA fire temperature, size, and power are dynamically scaled to the minima and maxima of the data.

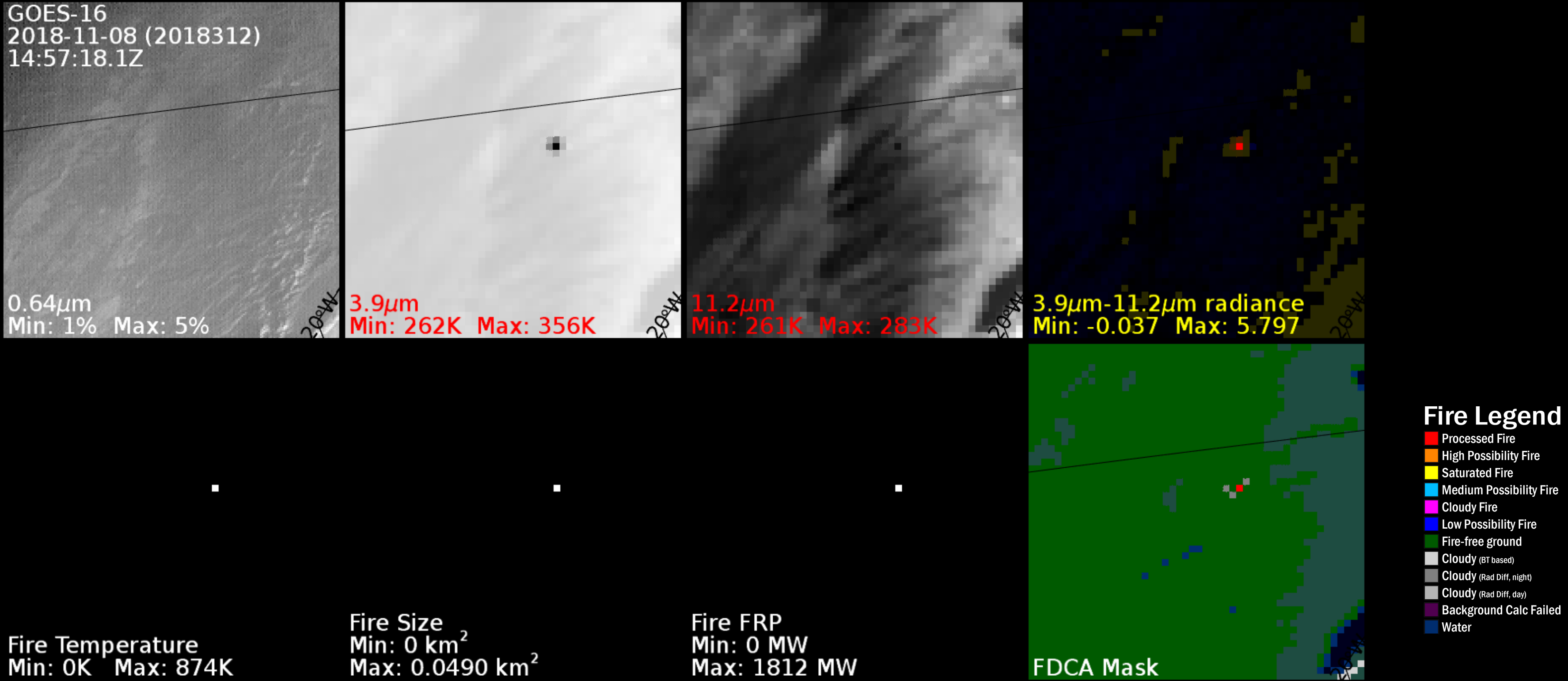

The Camp Fire

The visible, 3.9 µm, 11.2 µm, 3.9 µm minus 11.2 µm radiance difference in 3.9 µm radiance space, and FDCA fire temperature, size, and power are dynamically scaled to the minima and maxima of the data.

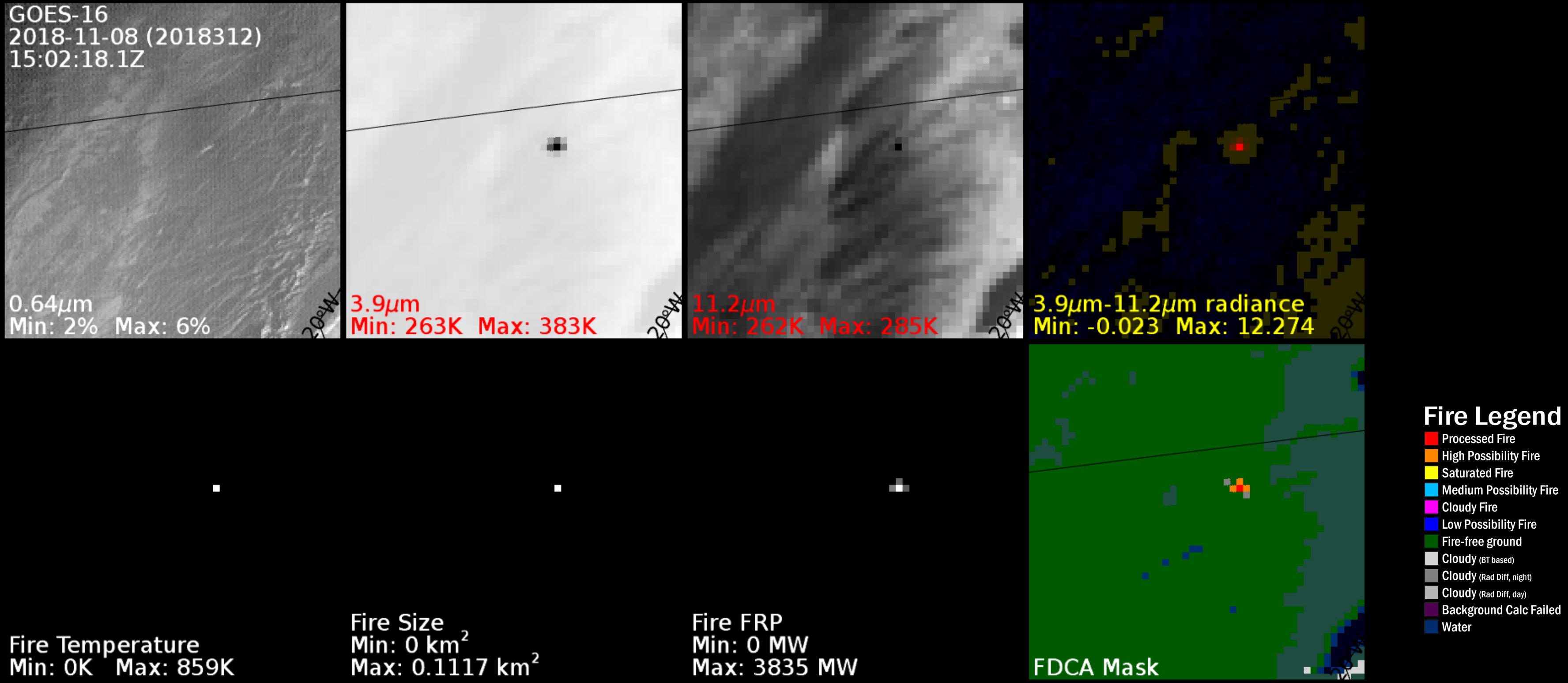

The Camp Fire

The visible, 3.9 µm, 11.2 µm, 3.9 µm minus 11.2 µm radiance difference in 3.9 µm radiance space, and FDCA fire temperature, size, and power are dynamically scaled to the minima and maxima of the data.

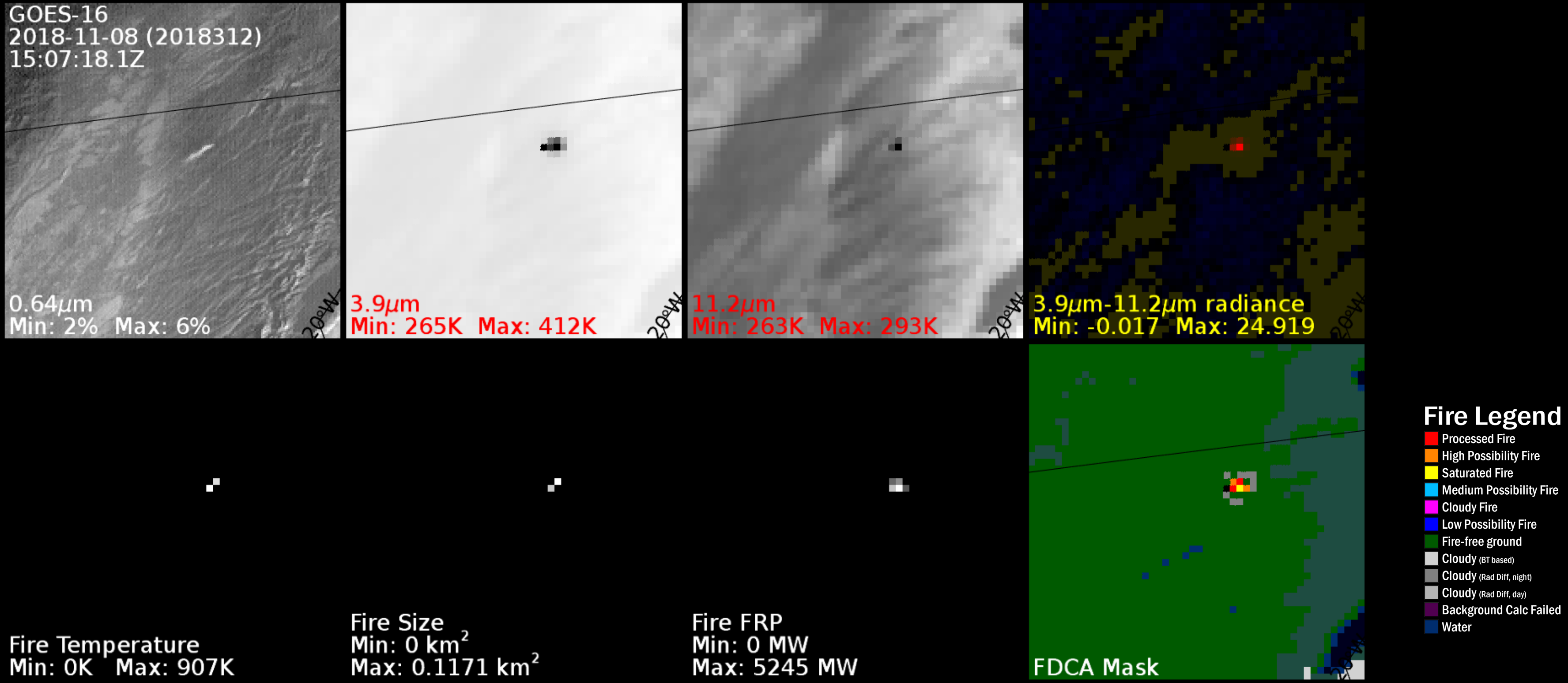

The Camp Fire

The visible, 3.9 µm, 11.2 µm, 3.9 µm minus 11.2 µm radiance difference in 3.9 µm radiance space, and FDCA fire temperature, size, and power are dynamically scaled to the minima and maxima of the data.

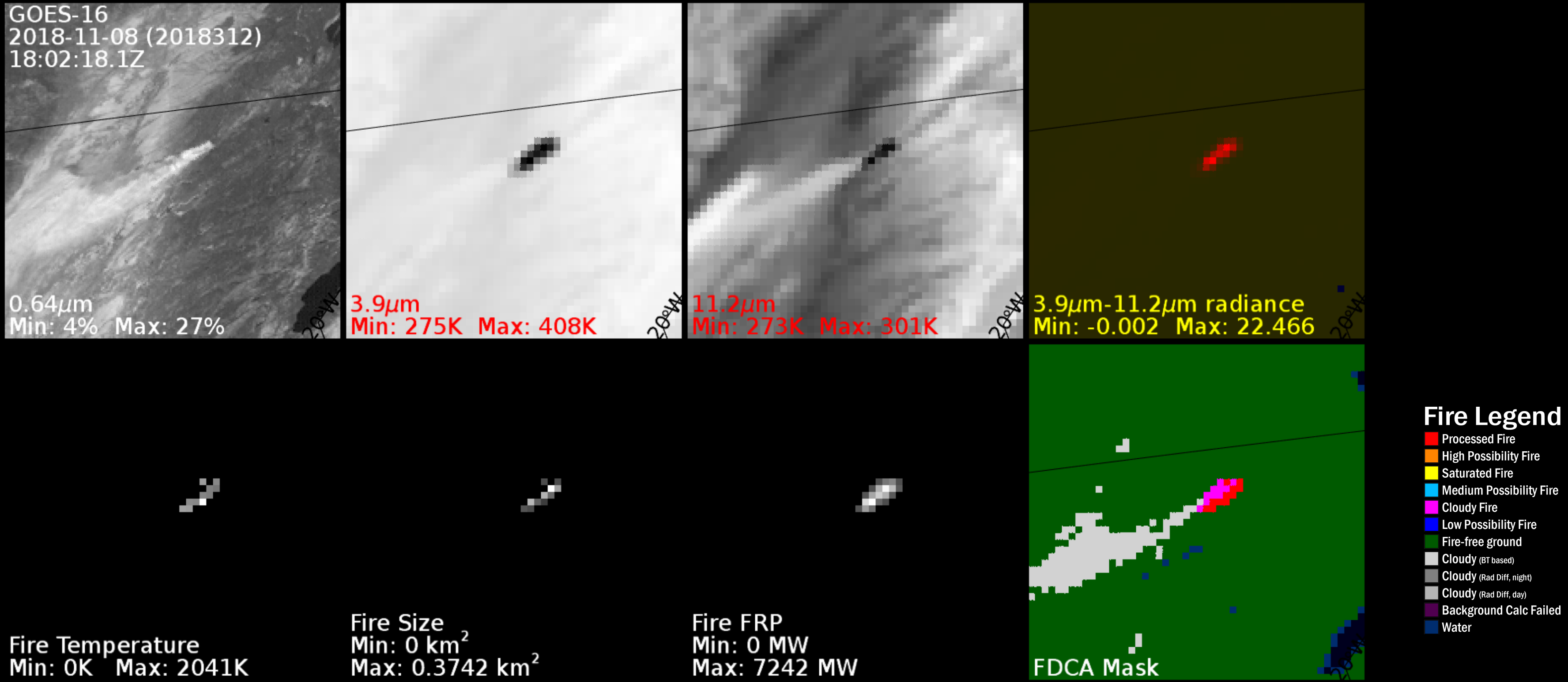

The Camp Fire

The visible, 3.9 μm, 11.2 μm, 3.9 μm minus 11.2 μm radiance difference in 3.9 μm radiance space, and FDCA fire temperature, size, and power are dynamically scaled to the minima and maxima of the data.

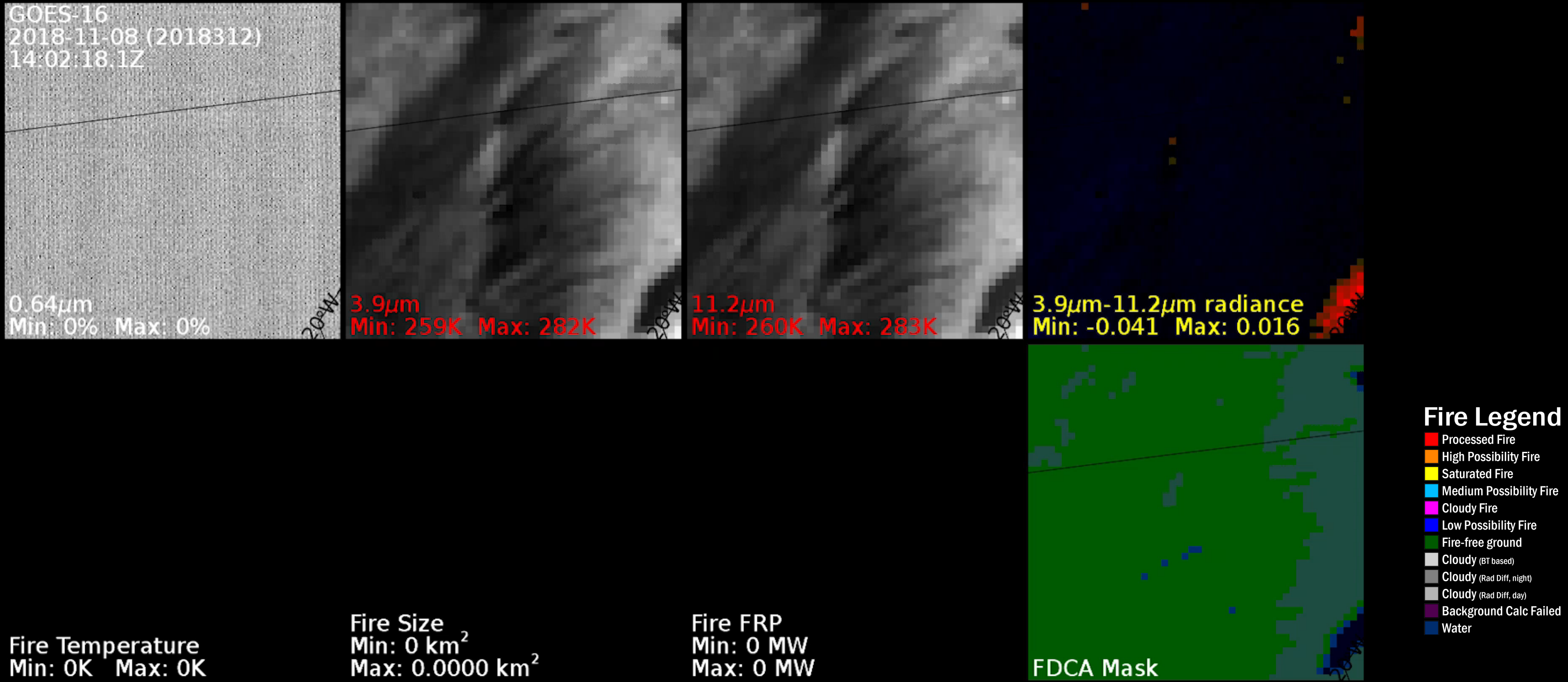

ABI Fire Sensitivity

On the evening of 24 February 2019, a NWS forecaster out of Green Bay was looking at 3.9 µm, imagery and saw a hotspot south of Oshkosh. Concerned that a major fire or perhaps plane crash had occurred, he called Winnebago County Emergency Services and learned that it was a house fire. The fire was called in at 10:17 pm CST, it was first visible in the mesoscale sector imagery at 10:39 pm CST.

AWIPS MESO sector loop courtesy Scott Lindstrom: http://cimss.ssec.wisc.edu/goes/blog/archives/32041

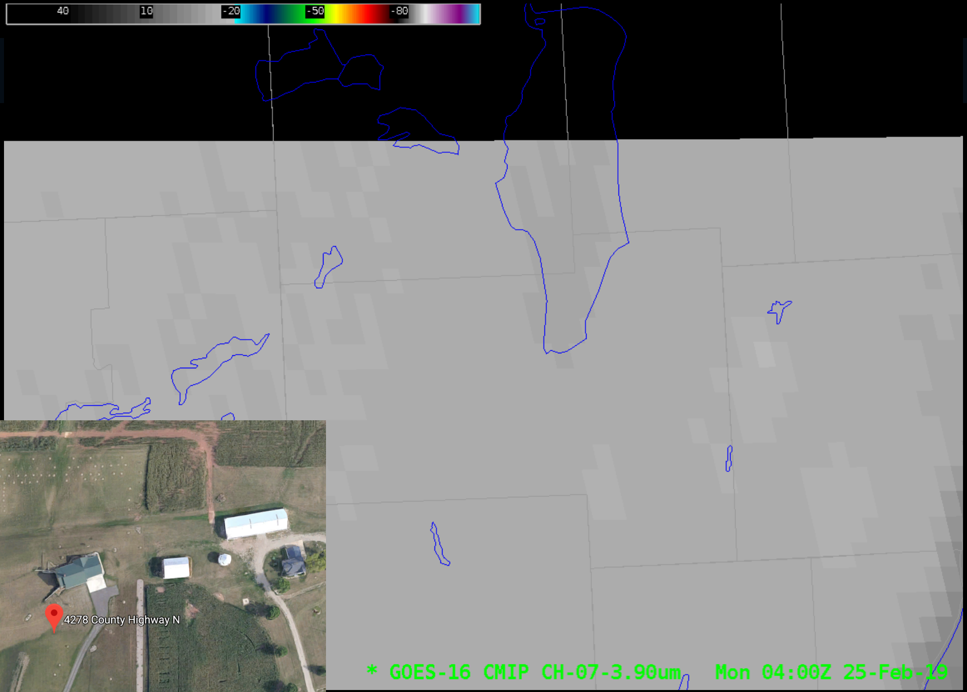

The Rhea Fire

Rhea Fire

12 April 2018, 16:00:29 UTC
to
13 April 2018, 23:59:29 UTC

1920 frames of fire data in 32 hours

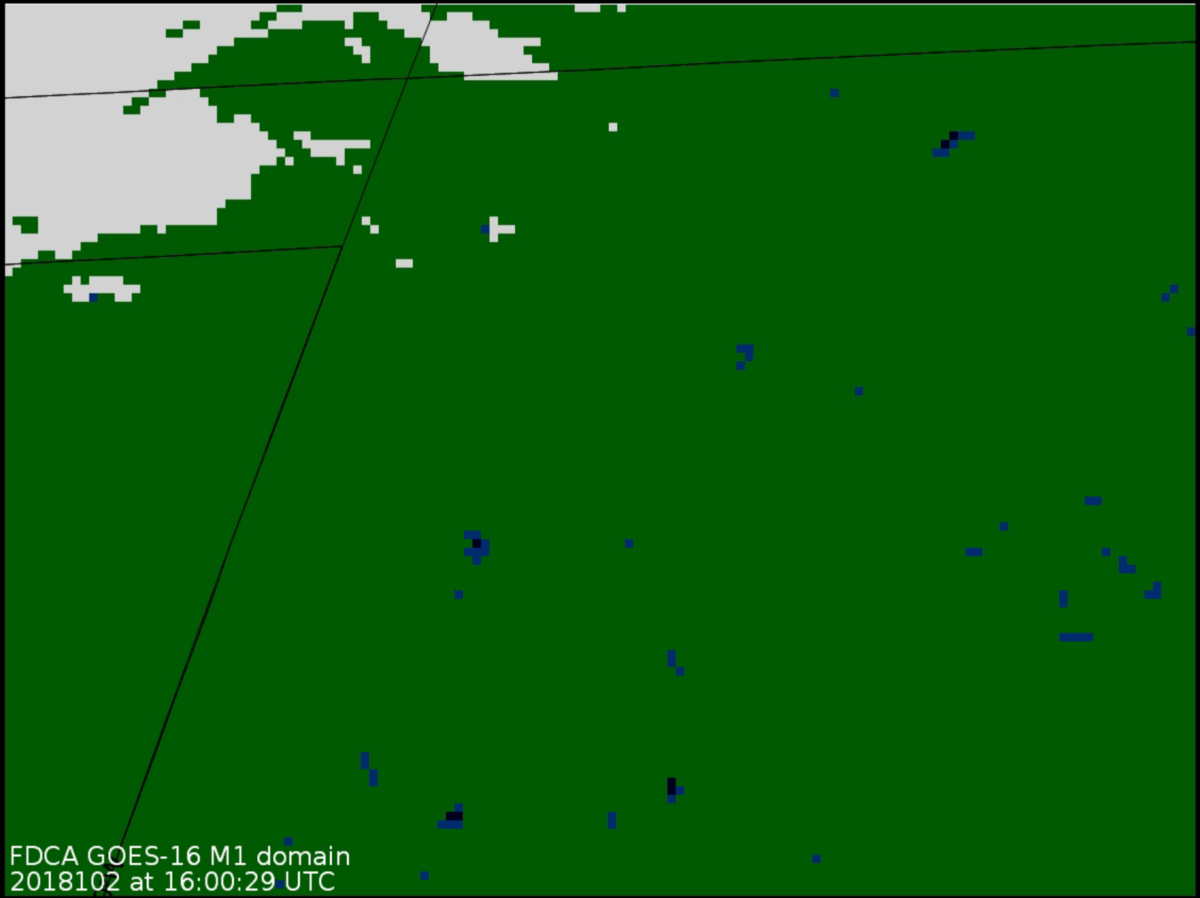

Fire Legend

- Processed Fire
- High Possibility Fire
- Saturated Fire
- Medium Possibility Fire
- Cloudy Fire
- Low Possibility Fire
- Fire-free ground
- Cloudy (BT based)
- Cloudy (Rad Diff, night)
- Cloudy (Rad Diff, day)
- Background Calc Failed
- Water

The Rhea Fire

Selected time steps of the fire product from the Rhea Fire.

Generally the product matches what we would expect to see based on the 3.9 µm band, except at 10 UTC when clouds interfered in the scene.

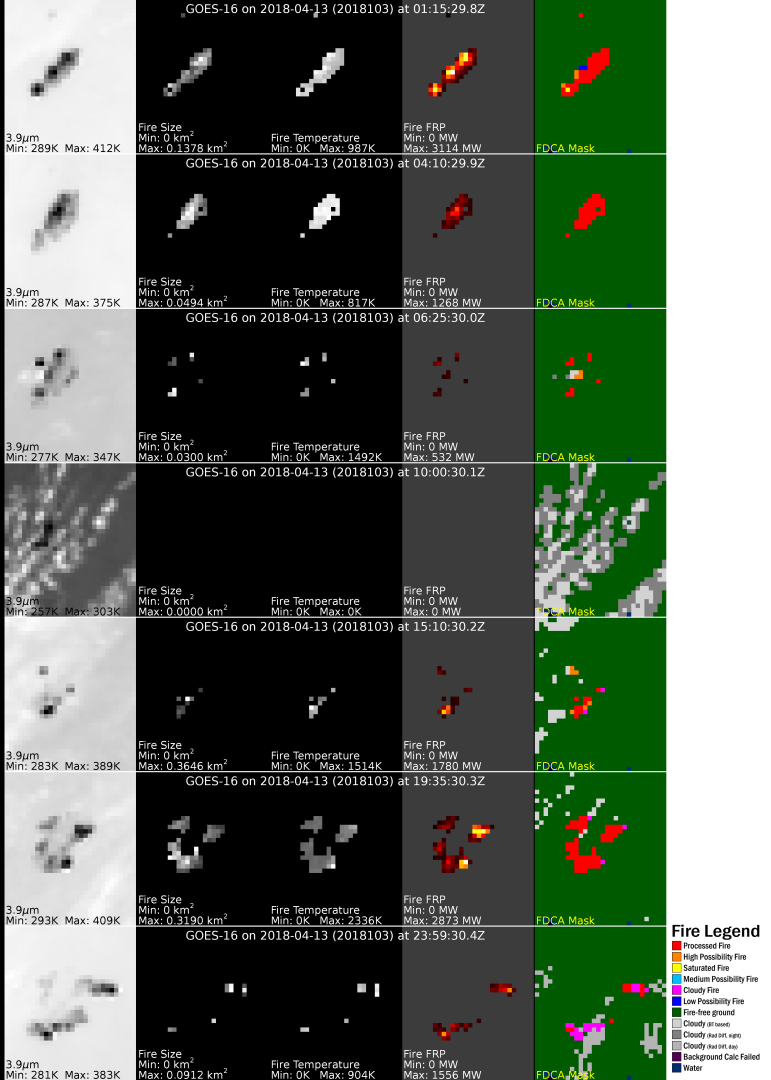

The Rhea Fire

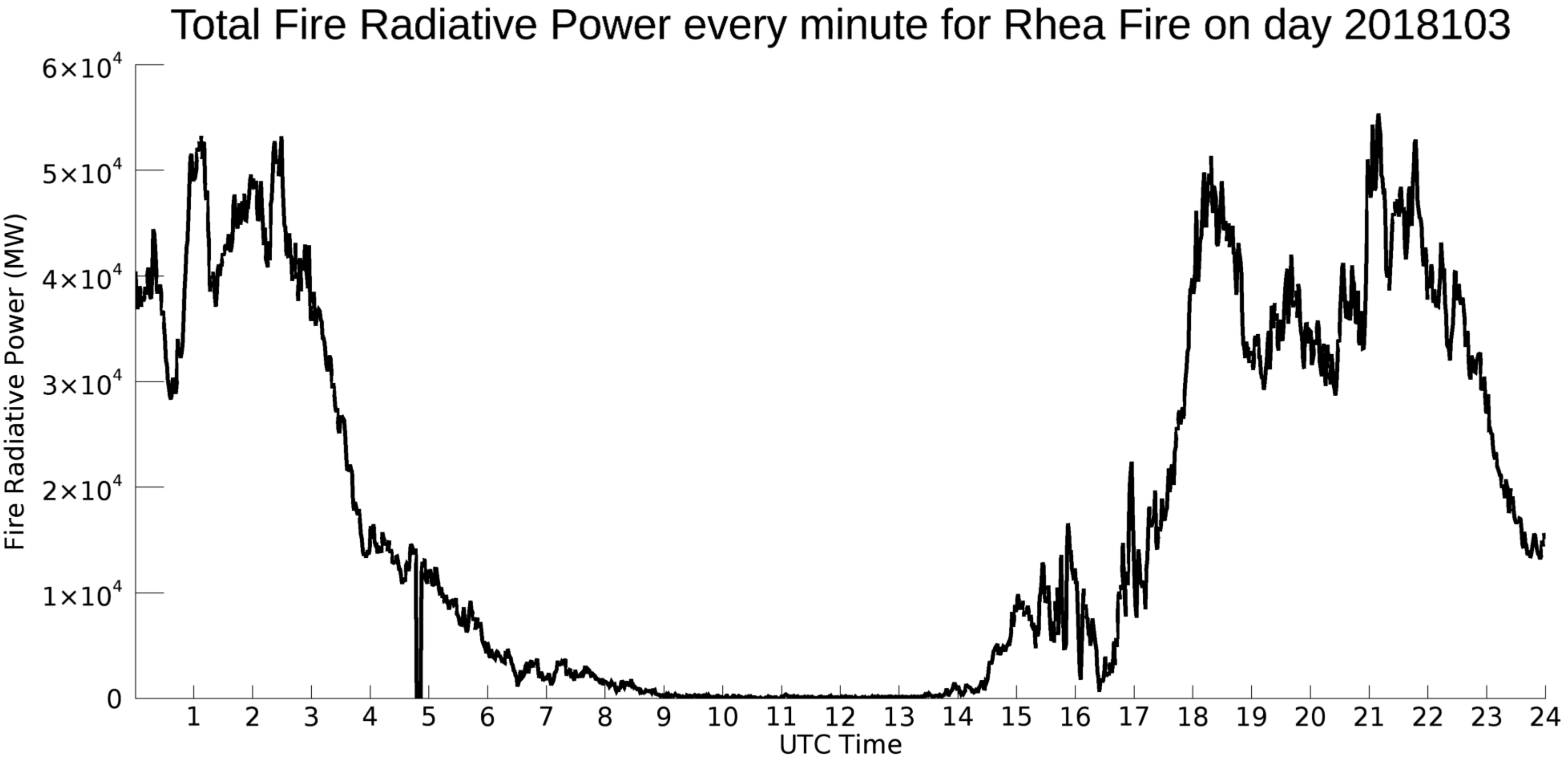

The Rhea Fire

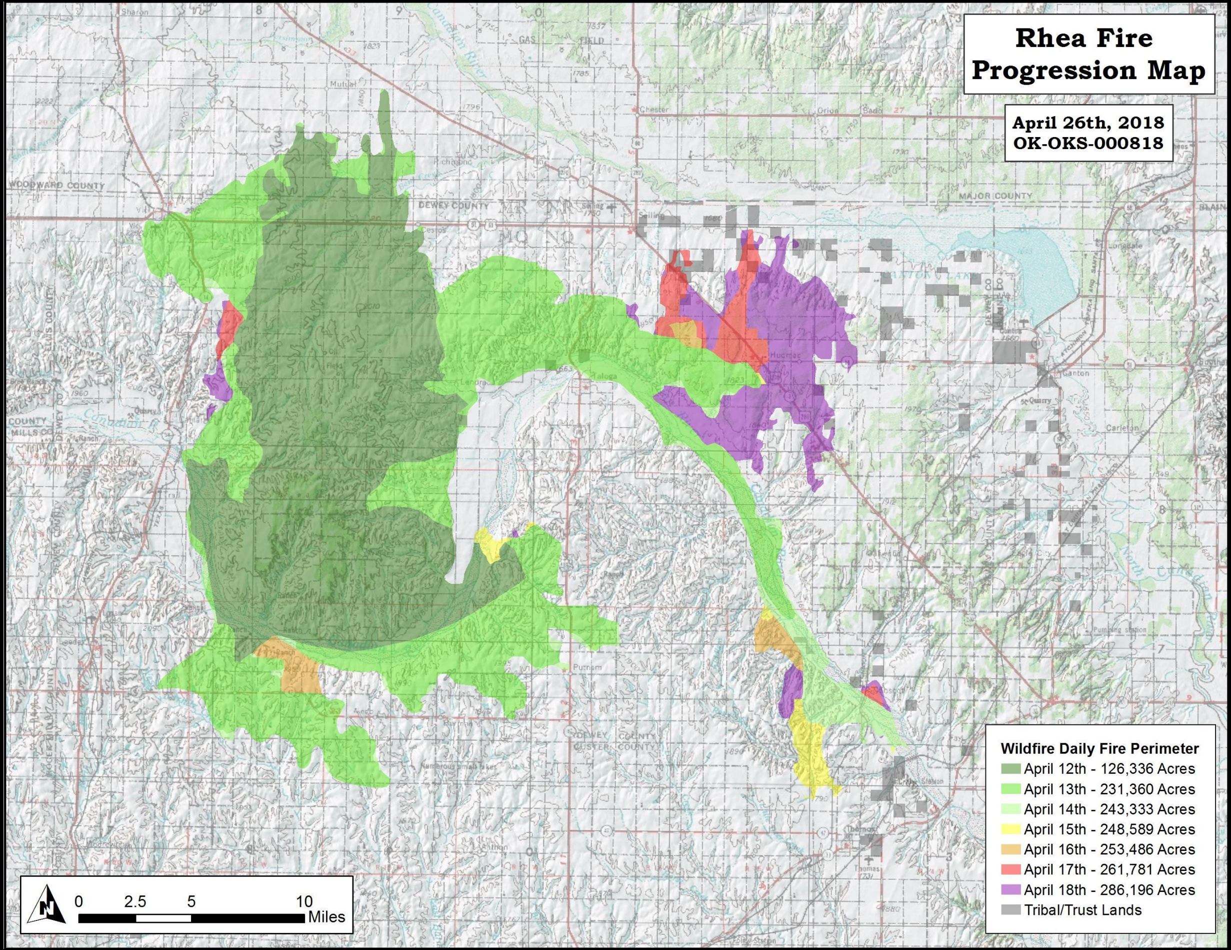

Image credit: Inciweb
https://inciweb.nwcg.gov/incident/5746/

Validation of Fire Detection and Characterization

There are few reliable datasets of fire occurrence, let alone properties. Those that do exist tend to be very limited in coverage in time and space, limited their utility for validation.

Fire locations from GOES ABI can be compared to those obtained from VIIRS and MODIS, as well as the smaller number of points from Landsat-class sensors. FRP can be compared between the polar platforms and GOES, though caveats apply. There is not a good way to validate the results of the Dozier Method, as they represent a hypothetical fire within that specific pixel. As a result, the standard for assessing its success is to verify that its results reproduce the input data.

For the purposes of GOES-R series validation, a hybrid approach is in use. Routine validation is done by a combination of visual inspection – essentially comparing the product outputs to the satellite imagery, and detection matchups against VIIRS and MODIS. So-called “deep dive” validation uses Landsat-class data (<50m pixels) to verify fire locations. FRP is being validated by comparison with results from MODIS and VIIRS. In general FDCA FRP is higher than from those satellites, which may reflect the “oversharpening” produced by the original remapping of ABI data. The remapping was changed in April 2019 and new results are not yet available.

Following FRP comparisons courtesy Shobha Kondragunta[1], Fangjun Li[2], and Xioayang Zhang[2]

1) NOAA/NESDIS/Center for Satellite Applications and Research

2) Geospatial Sciences Center of Excellence, South Dakota State University

FRP Comparison, Time Series (3/24/2018)

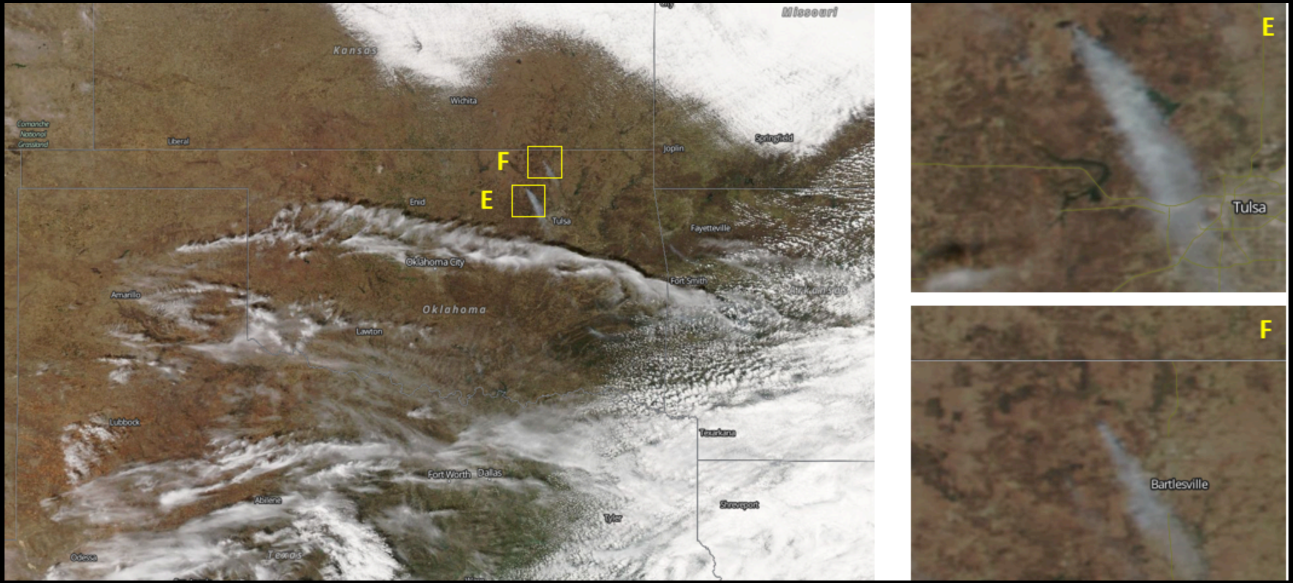

FRP Comparison, Time Series (3/24/2018)

FRP Time Series (E)

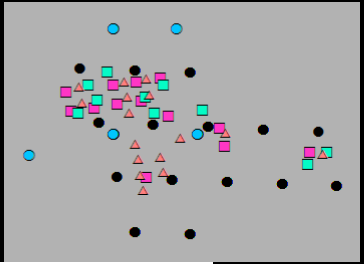

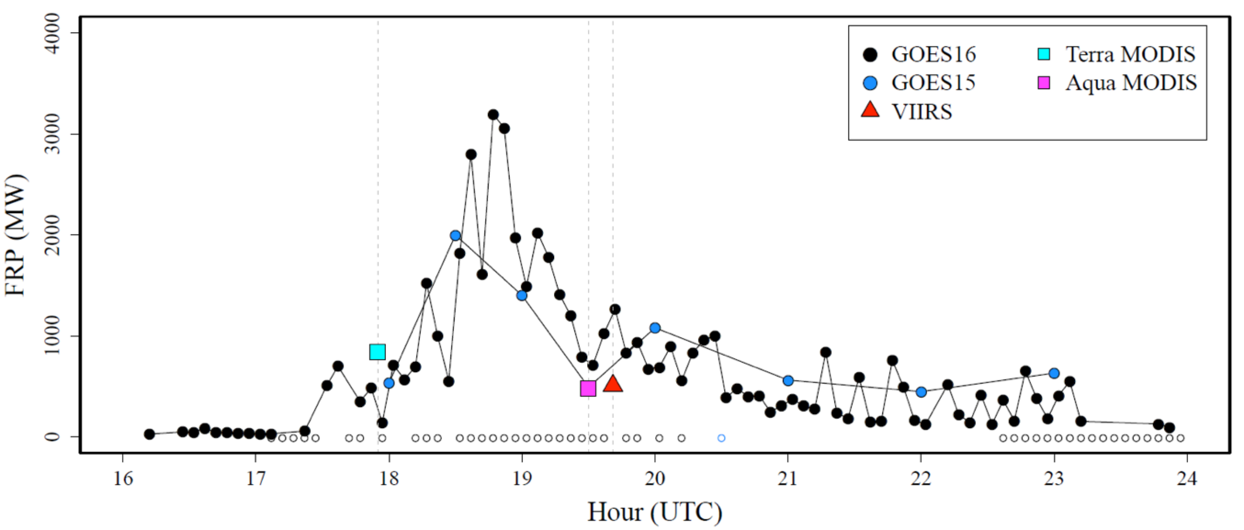

FRP Comparison, Time Series (3/24/2018)

FRP Time Series (F)

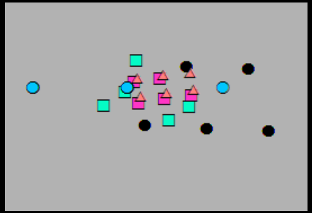

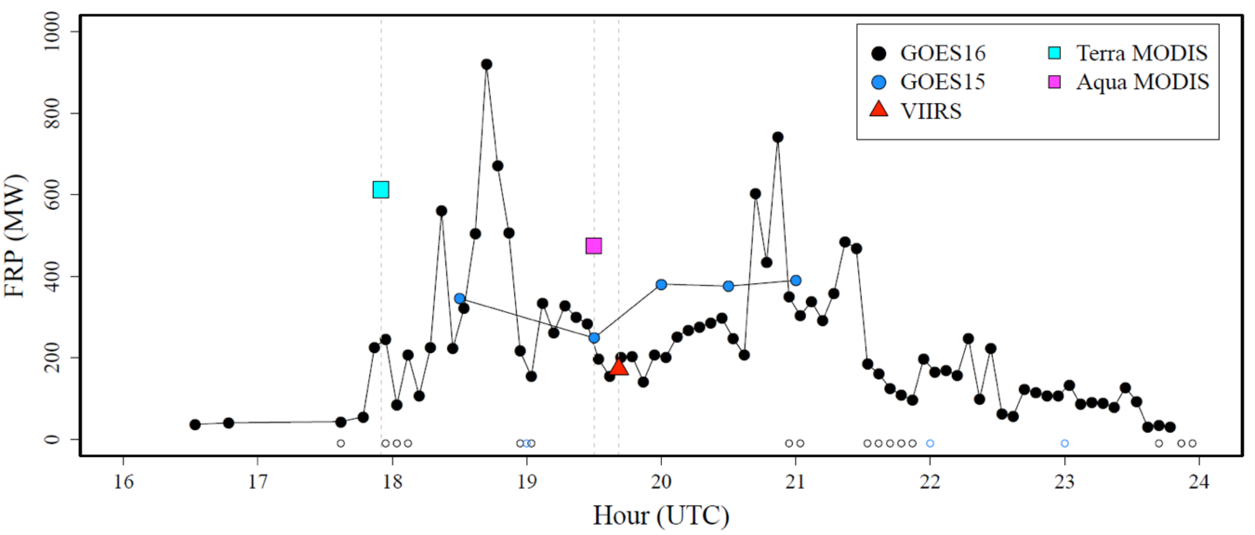

Good agreement for E and F between GOES-16, GOES-15, and VIIRS – these are generally flat locations. Unclear why MODIS disagrees a fair amount.

FRP Comparison, Time Series (3/14/2018)

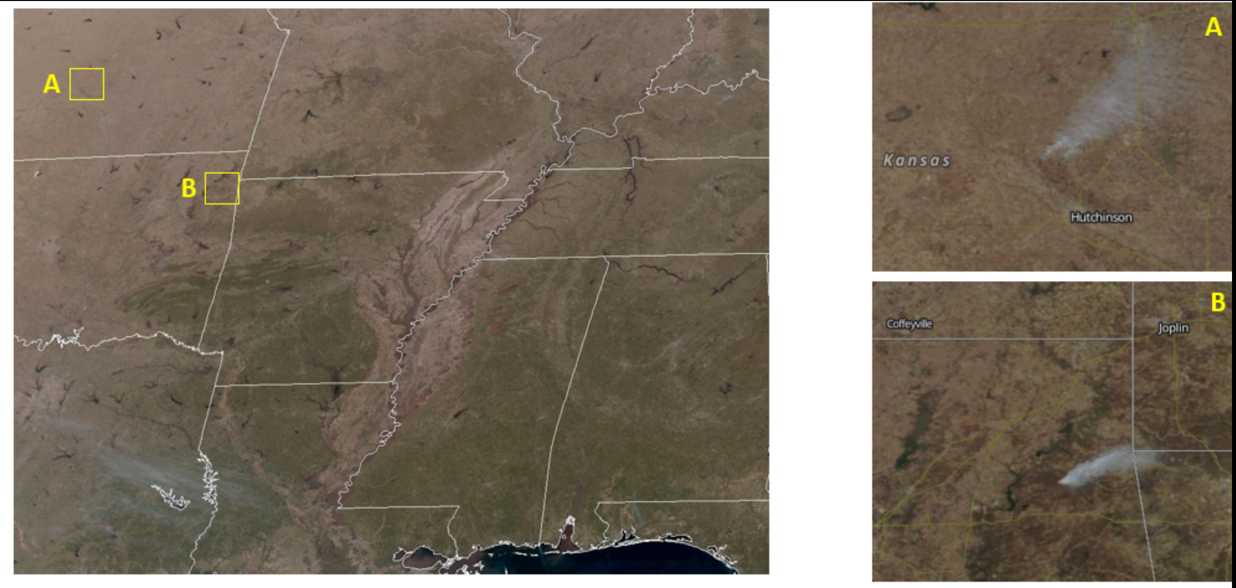

FRP Comparison, Time Series (3/14/2018)

FRP Time Series (A)

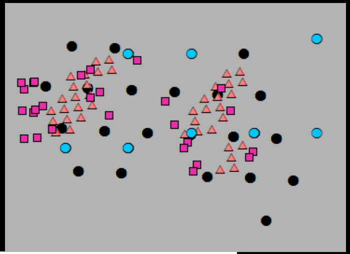

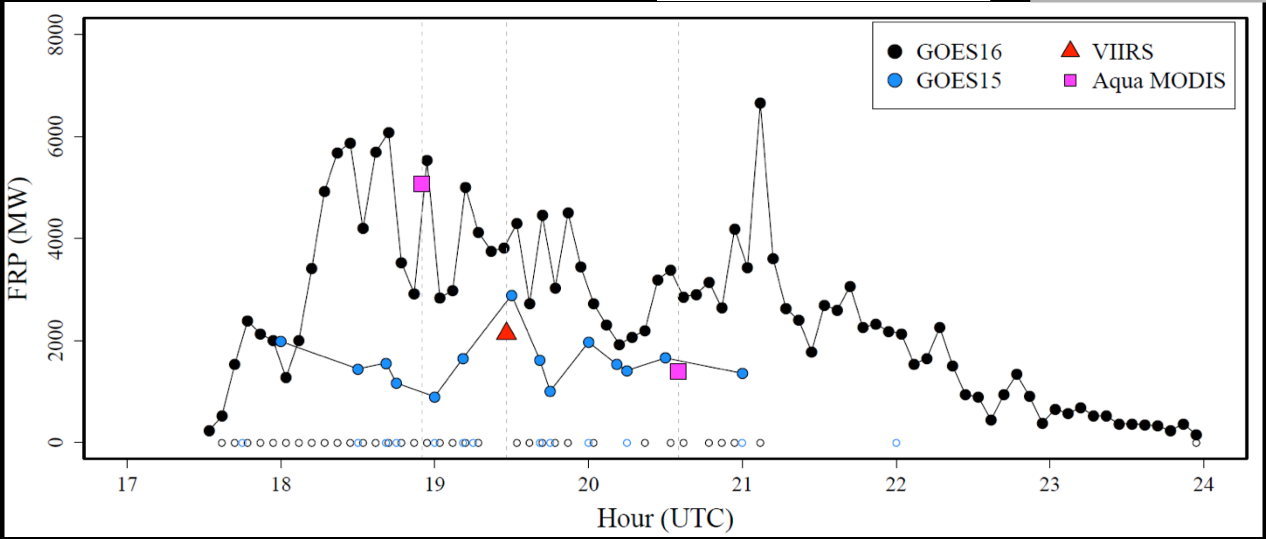

Agreement is not great, but not awful – could be due to multiple factors.

FRP Comparison, Time Series (3/14/2018)

FRP Time Series (B)

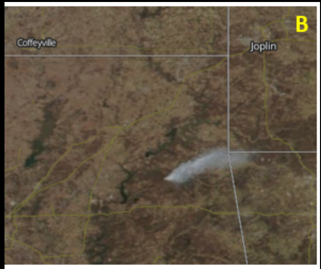

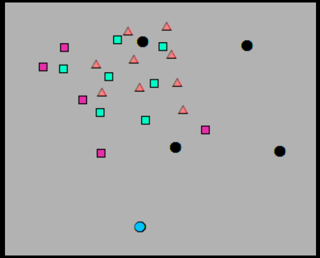

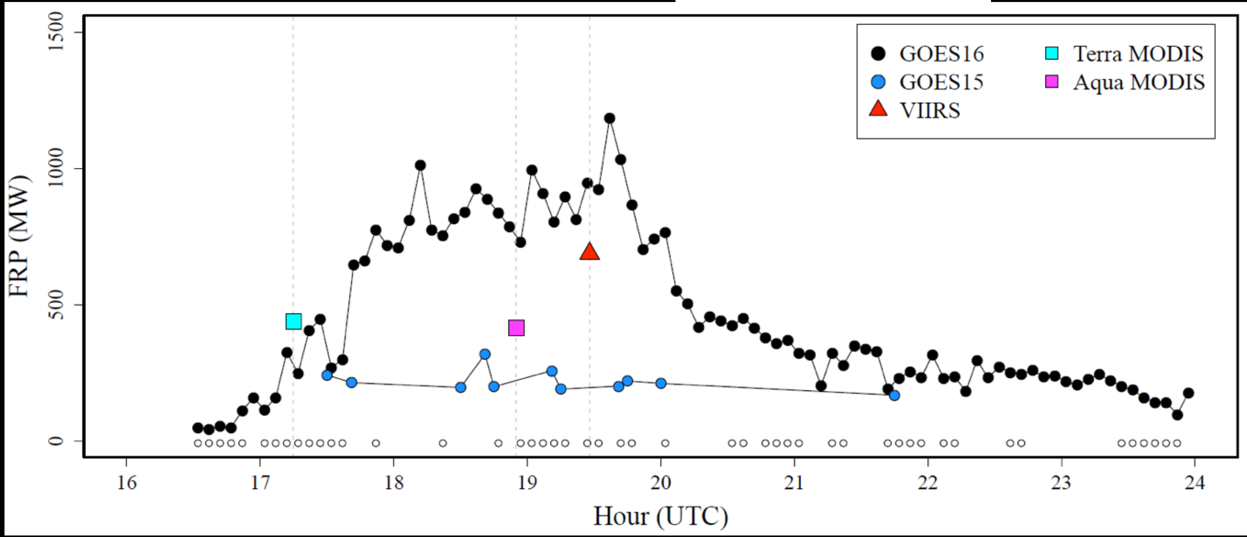

Notably poor agreement between G16 and G15 - Why?

FRP Comparison Between Platforms

3.9µm data, GOES-16 on the left, GOES-15 on the right
The fire in question (inside the yellow circles) looks very different – why?

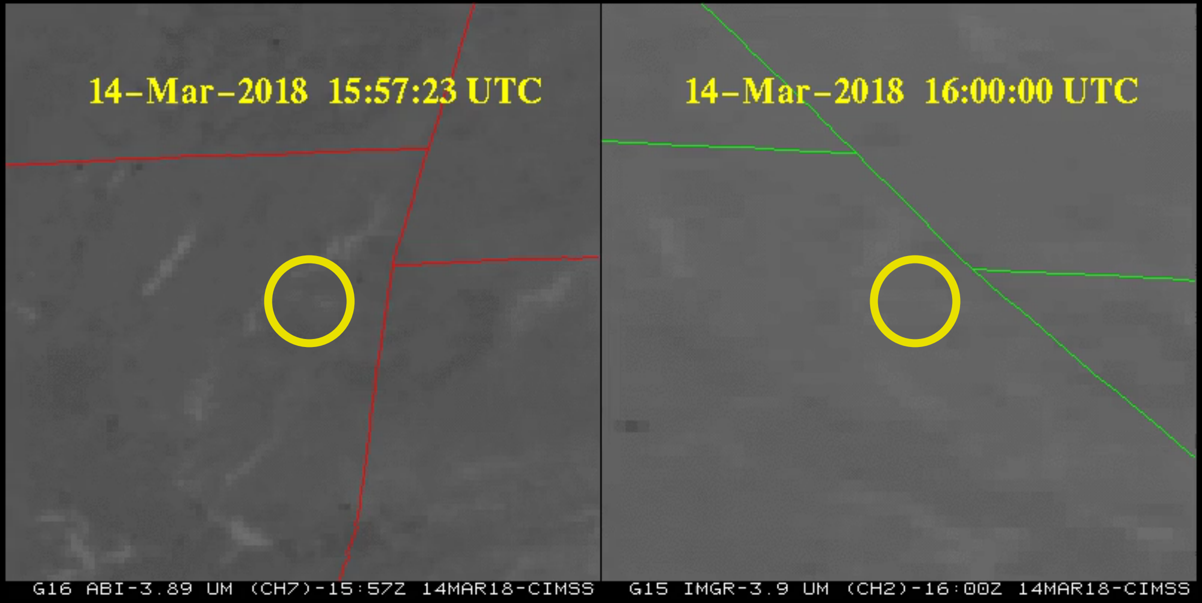

FRP Comparison, Time Series (3/14/2018)

Location B is in the Spavinaw Wildlife Refuge, and the hills generally slope to the east, north, and south. The view from the west is somewhat screened by the terrain, causing GOES-15 to have a poor view of the fire.

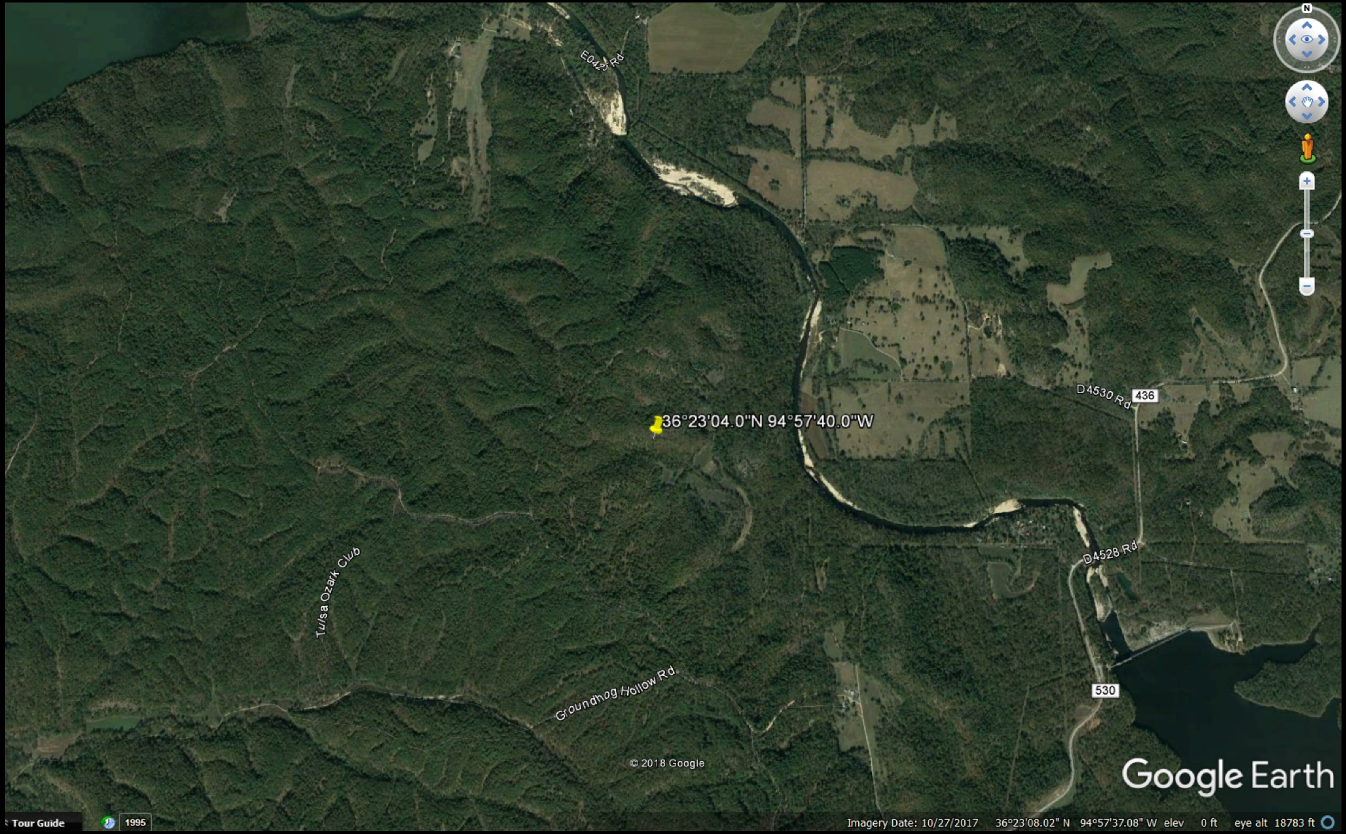

ABI Fire Detection Wrap-up and Caveats

Initial version of algorithm inherited the WFABBA's tendency to produce false alarms during the day, particularly when water clouds were involved and near sunrise and sunset. An update that largely eliminates that problem is in the process of being implemented in the GOES-R Ground System, expected to be live in June 2019. All results shown in this presentation were produced with the new version of the algorithm.

There are known false alarms caused by solar power plants and reflective ground surfaces.

Algorithm performance for cold backgrounds is currently diminished, if the brightness temperature is below about 270 K the algorithm generally ignores the pixels, which has led to missing a large number of fires during the colder months.

Bright reflective surfaces can be inadvertently be flagged as cloudy.

Fixes for these issues are in development.

Algorithm will reach full validation, at which point the above issues and GOES-17 problems mitigated, some time in 2020.

The End

Contact email:

chris.schmidt@ssec.wisc.edu

Special thanks to:

Ivan Csiszar (NOAA)
Wilfrid Schroeder (NOAA)
Joanne Hall (UMD)
Shobha Kondragunta (NOAA)
Fangjun Li (GSCE)
Xiaoyang Zhang (GSCE)
Jim Nelson (CIMSS)
Mat Gunshor (CIMSS)
Tim Schmit (NOAA)

Backup Slides

Planck Curves

Instruments like ABI, the old GOES Imager, MODIS, and VIIRS can detect fires. Algorithms for all of them primarily rely on a band at ~4 μm compared to a band at ~11 μm, taking advantage of the behavior of the Planck function. As an emitter heats up, its peak emission moves to shorter wavelengths.

Many bands can "see" fire signals, but around ~4 μm is best suited because for the range of temperatures at which biomass burns, the strongest response occurs at ~4 μm. That wavelength is mostly, but not completely, out of the range of influence of reflected sunlight, and relatively unaffected by water vapor, though a correction is still needed to account for attenuation when calculating properties.

Fires are generally much smaller than the pixel itself, occupying a few percent of the footprint at most. They are still detectable because the burning portion emits one or more orders of magnitude more radiance than its surroundings at ~4 μm.

Note: Diffraction causes an uneven response across the pixel footprint, giving a higher weight to energy coming from the center of the pixel than it does to energy from the fringes. That leads to a fundamental limit to the ability to characterize fire properties.

Planck Curves

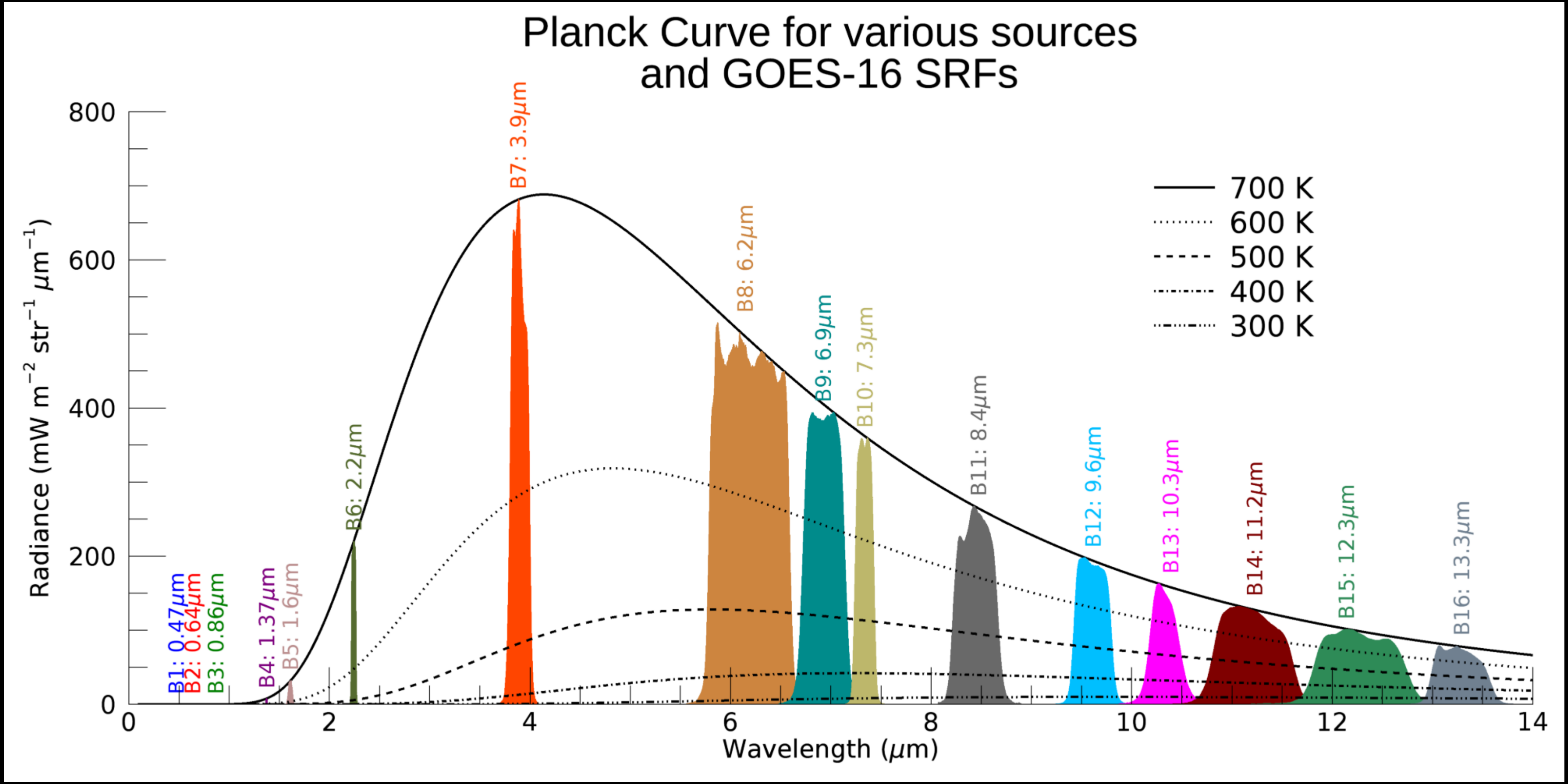

Planck Curves

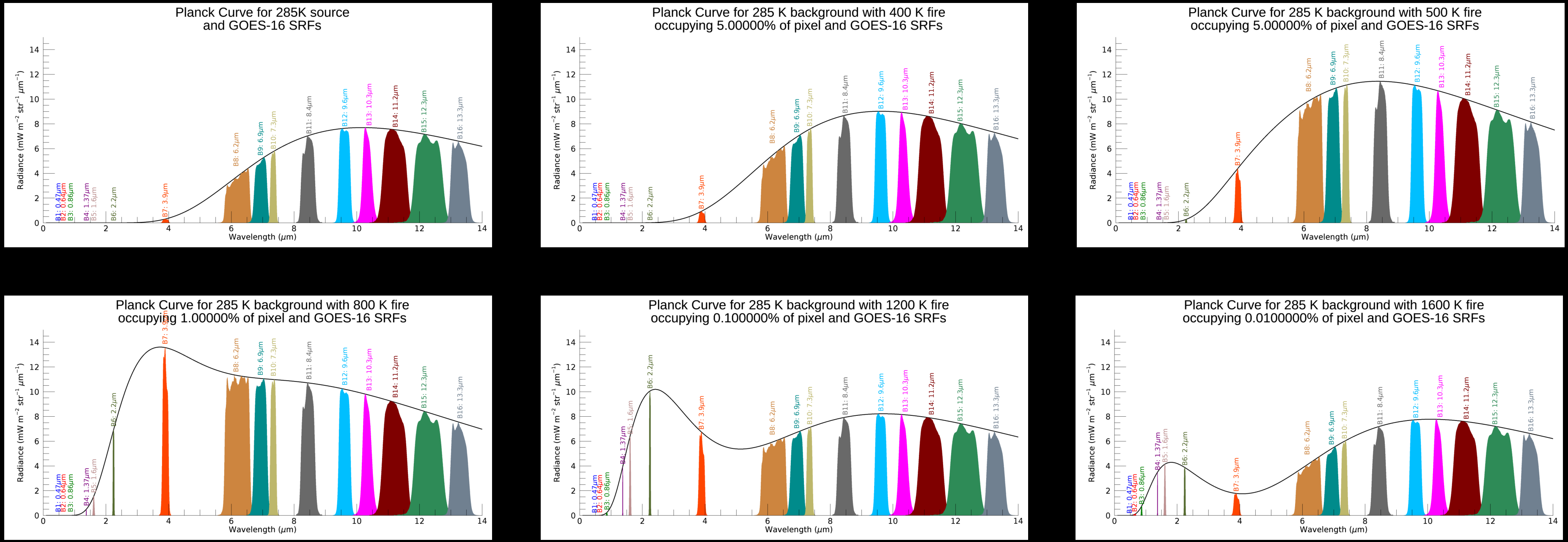

Planck curves for various combinations of fire temperature and pixel fraction. The background is held at 285 K in all cases. The calculations assume that the pixel fraction that is burning is of uniform temperature and there is no diffraction. A real fire contains a range of burning conditions: different temperatures, different emissivities, different attenuation due to smoke and water vapor variations on small scales, variations in terrain changing how the satellite sees the fires, and so on.

Fire Characterization

While fire detection is important, quantitative applications such as smoke modeling need to know how energetic the fire is. The original ABBA was designed to provide fire size and fire temperature using a relationship described by Matson and Dozier that correlated the fire temperature and pixel fraction with the observed radiances in the ~4 μm and ~11 μm bands. Later on, fire radiative power (FRP) caught on as a simplified way to assess a fire's character.

Due to the subpixel nature of fires, the Dozier Method and FRP are describing a hypothetical, uniform fire with those properties that produces the same radiance signature. The size in particular should not be taken literally.

Fire Products: Fire Size and Temperature

Estimated with two simultaneous equations (aka the Dozier Method):

+ +

+

The equations are solved for and .

Combined with pixel size, the method yields quantities that can be used to estimate emissions. This method predates FRP and some models still use it.

The size and temperature represent a hypothetical fire of that size and uniform temperature that would produce the same radiance signal. They should not be used independently.

L_4	4 µm observed radiance
L_{11}	11 µm observed radiance
L_{4s}	4 µm reflected solar radiance term
p	proportion of pixel on fire
1-p	proportion of pixel not on fire
T_4	4 µm observed brightness temperature
T_{11}	11 µm observed brightness temperature
T_b	Background/non-fire brightness temperature
T_t	Average instantaneous target temperature of sub-pixel fire
τ_{4s}	Transmittance of the 4 µm solar term
ε_4	4 µm emissivity

Fire Products: Fire Radiative Power (FRP)

Physical definition of power:

A = Area
T=Blackbody temperature,
ε=Emissivity
σ=Stephan-Boltzman Constant

For a mixed pixel of fire and non-fire:

Approximation using radiances:

L_{MIR}	4 µm observed radiance	p_k	Instantaneous proportion of pixel on fire
$L_{B,MIR}$	4 µm calculated background radiance	T_k	Instantaneous target temperature of sub-pixel fire
A_{sample}	Area of pixel	ε	Emissivity of fire (typ. assumed to be 1)
a	A constant (function of instrument SRF)	σ	Stefan-Boltzmann constant

Using FRP: